Fundamentals of gamma spectrometry

γ-SPEKT/GRUNDL

Authors:

D. Arnold [1]

K. Debertin† [1]

A. Heckel [2]

G. Kanisch [3]

H. Wershofen [1]

C. Wilhelm [4]

[1] Physikalisch-Technische Bundesanstalt
(Physikalisch-Technische Bundesanstalt)

[2] Federal Office for Radiation Protection
(Bundesamt für Strahlenschutz)

[3] Thünen Institute of Fisheries Ecology
(Thünen-Institut für Fischereiökologie)

[4] Karlsruhe Institute of Technology
(Karlsruher Institut für Technologie – KIT)

ISSN 1865-8725 Version March 2018

Procedures Manual for monitoring of radioactive substances in the environment and of external radiation
(Messanleitungen für die „Überwachung radioaktiver Stoffe in der Umwelt und externer Strahlung“)

C O N T E N T

ISSN 1865-8725 Version March 2018

A N N E X E S

ISSN 1865-8725 Version March 2018

Fundamentals of gamma spectrometry

1 Introduction

Gamma spectrometry plays a key role for monitoring radioactive substances in the environment, since a number of natural radionuclides as well as fission and activation products from nuclear plants emit gamma radiation.

The advantages of gamma spectrometry are, among other things, that it allows the simultaneous identification and activity determination of different radionuclides in one counting source. Most of the time, the counting sources can be produced from the most various matrices without demanding sample processing. The relevant energy region of the gamma-emitting radionuclides to be detected ranges from approx. 30 keV to approx. 2000 keV. With this procedure, it is possible to detect low activities of radioactive substances down to 0,1 Bq with sufficient certainty.

The following sections will provide information about

— the setup of a gamma spectrometric measurement system,

— its calibration,

— the evaluation of pulse height spectra, and

— the activity determination.

As physical basics of gamma spectrometry and detailed functionalities of the detectors and electronic units are beyond the scope of this General Chapter, it is referred to the relevant literature [1, 2, 3] for more information.

2 Components of a gamma spectrometric measurement system

A gamma spectrometric measurement system essentially consists of four components (see Figure 1):

— the detector (see Section 2.1),

— the detector shielding (see Section 2.2),

— the electronic unit (see Section 2.3), and

— the computer including its software (see Section 2.4).

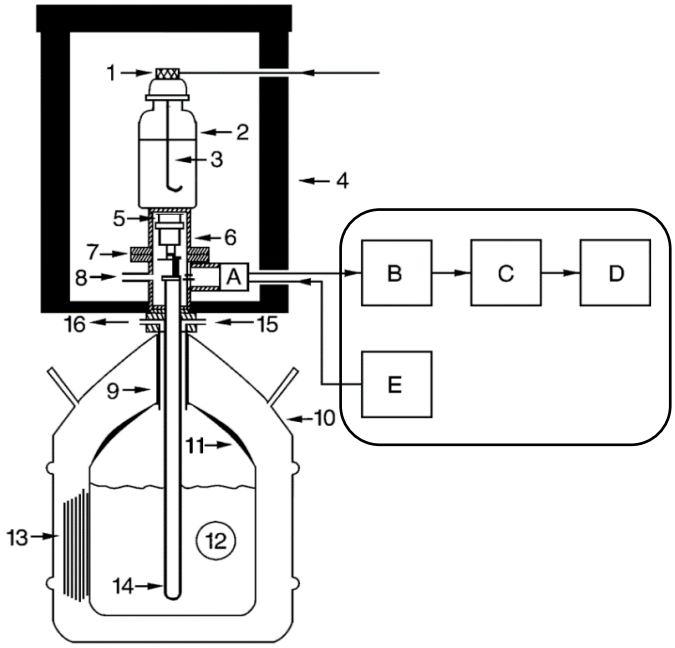

1 Stirrer motor
2 Polyethylene bottle
3 Stirrer (e.g. silicone tube)
4 Lead shielding
5 Detector
6 End cap
7 Flange connection
8 Vacuum exhaust nozzle
9 Necktube
10 Dewar container
11 Molecular sieve
12 Nitrogen (liquid)
13 Insulation
14 Cooling rod (copper)
15 Inlet nozzle for liquid nitrogen
16 Vent

A Pre-amplifier
B Main amplifier
C Multichannel analyser
D Spectra evaluation and documentation
E Current and high-voltage source

Fig. 1: Schematic representation of a measurement system for gamma spectrometry with an aqueous counting source

2.1 Detector

2.1.1 Detector material

Detectors for gamma spectrometry are differentiated according to the materials used for the detector and to the construction type.

Today, the following detector materials are used for gamma spectrometric measurements:

— NaI(Tl);

— $LaBr_3$;

— Si(Li);

— High-purity germanium (HPGe).

Due to their relatively low energy resolution capability, gamma spectrometers with NaI(Tl) or $LaBr_3$ are mainly used for, i. e. screening procedures, in mobile measurement systems or for dose or absorbed dose rate measurements.

In contrast, Si(Li) detectors are suitable in gamma spectrometry to determine the activity of X-ray and low-energy gamma-rays with photon energies below 60 keV.

Radioactive substances are mainly measured using HPGe detectors due to their high energy resolution. This allows a simultaneous determination of different radionuclides in

the same counting source. Two different types of HPGe detectors are differentiated, depending on the material their crystal is doped with: p-type germanium is doped with trivalent elements (e. g. boron), whereas n-type germanium is doped with pentavalent elements (e. g. phosphor). The standard designs of these two detector types differ with regard to the thickness of their dead layer on the entry side of the radiation. In case of n-type detectors, this layer is thinner, which explains why they are better suited for the measurement of low-energy gamma-emitting radionuclides (see Section 6.3).

Components located in the immediate vicinity of the crystal (e. g. the crystal holder, the end cap with the entrance window and pre-amplifier components) must be selected in such a way that disturbances due to the activity of natural or artificial radionuclides in the material of these components are minimized (see General Chapter γ-SPEKT/NULLEF of this Procedures Manual).

2.1.2 Crystal form

The detector materials mentioned are manufactured as crystals in different designs:

— planar crystal;

— coaxial crystal;

— special forms (e. g. borehole crystal).

The diameter of planar crystals is greater than their height. These crystals are therefore well-suited for the measurement of flat counting sources. Due to their low height, these crystals have a lower efficiency for higher-energy gamma radiation than coaxial crystals.

The diameter and height of coaxial crystals are similar. Therefore, they are better suited for the measurement of counting sources with a greater volume and the activity determination of higher-energy gamma-emitting radionuclides.

These are the most frequently used designs, but there are also special forms. Borehole crystals are one of these special forms worth mentioning. A borehole crystal is a coaxial crystal with a borehole along the longitudinal axis that reaches approximately the centre of the crystal. The counting source is inserted in this borehole. When there is only a small amount of sample material available or if the counting source has been reduced to a small volume, borehole crystals provide particularly high detection efficiency.

2.1.3 Operating high-purity germanium detectors

HPGe detectors are operated at high voltage and must be cooled down to very low temperatures before commissioning. Cooling is achieved either using liquid nitrogen or an electric cooling system. Permanent cooling is strongly recommended to ensure long-term stability of the crystal, since this minimizes changes in its dead layer due to diffusion.

After longer operation breaks or after repair causing the crystal to reach room temperature, its detector properties should be checked when re-commissioning the crystal.

Note:
Changes in the efficiency must be expected in particular in the low-energy range.

The most basic design with regard to cooling systems (cryostats) based on liquid nitrogen consists of the components 9 to 16 in Figure 1. Positioning the crystal in relation to the cryostat may be carried out in different ways: depending on the purpose of the measurement and on the space available, one may choose to position the crystal vertically or at a tilt in relation to the cryostat. In the case of the easiest arrangement, the crystal is placed on top of a vertical dipstick in the dewar, as shown in Figure 1. Horizontally tilted cryostats require longer dipsticks and thus have a higher liquid nitrogen consumption.

The technical design of the crystal/cryostat ensemble must minimize the transmission of mechanical vibrations (e. g. sound or oscillations of buildings) onto the detector system as much as possible. This effect is called microphony and influences the energy resolution of the spectrometer. For example, an elastic support or a vibration damper placed under the dewar considerably reduces this effect.

2.1.4 Detector parameters

The most important parameters of a detector are its sensitivity, its energy resolution capability, and the peak-to-Compton ratio. These parameters are determined for the gamma radiation emitted by Co-60 at 1332,5 keV and documented in the datasheet of the detector by the manufacturer.

The sensitivity – designated as "relative efficiency" in the datasheet – is defined as the ratio of the efficiency of the detector considered to that of a reference detector and stated in percent [4, 5]. Detectors are therefore available with a sensitivity of 100 % and more.

To detect radioactive substances in the environment, coaxial detectors with a sensitivity of approx. 25 % are sufficient – this corresponds to a crystal volume of approx. 100 cm^3. Depending on the application, detectors with superior sensitivity are used as well. Other conditions may apply to planar detectors.

Note:
The reference detector is defined as a cylindrical NaI(Tl) crystal with the following dimensions: 3'' x 3'' (7,62 cm) (height and diameter). To determine the efficiency of this detector, a point-like radiation source of known activity is measured on the central axis at a distance of 25 cm to the detector's end cap. The efficiency of the reference detector is $1{,}2 \cdot 10^{-3}$.

The full width at half maximum of the Co-60 gamma peak is used to determine the energy resolution. In modern detectors, its value is between 1,5 keV and 2,0 keV, depending on the design.

Note:
The full width at half maximum is a function of the gamma-ray energy and increases with the energy (see Section 6.2). At 100 keV, its value is 1,0 keV or less, depending on the design.
In addition, the full width at tenth maximum is stated in the detector data sheet. This is a measure of the deviation of the peak shape from that of a Gaussian function. Ideally, the full width at tenth maximum is 1,82 times the full width at half maximum.

The peak-to-Compton ratio is defined as the quotient of the amplitude of the full energy peak of Co-60 at 1332,5 keV by the average number of counts of the Compton spectrum in the range between 1040 keV and 1096 keV. Generally, the ratio increases with increasing crystal size. When comparing two crystals of the same size and of the same design, the peak-to-Compton ratio increases with increasing energy resolution capability.

2.1.5 How to select a suitable detector

Depending on the measurement purpose, different detector requirements arise when acquiring, modernizing or optimizing gamma spectrometric measurement systems. The following criteria must be taken into account when selecting a detector:

— Number of samples to analyse and requirements placed on the detection limit in routine and emergency operation of the respective measurement program;
— Sample matrix and geometry of the counting sources;
— Energy region of the photons emitted by the considered radionuclides;
— Detector properties (e. g. crystal material, crystal type, parameters);
— If relevant: spatial and technical infrastructure available.

From the information provided above, it is obvious that no unique detector is available being equally well-suited for all measurement tasks. Generally, choosing the largest possible detector with a very high energy resolution capability and a high peak-to-Compton ratio is recommended. The materials of the components located close to the detector should be as free of radioactive impurities as possible.

Note:
The continuum in the pulse height spectrum below 1200 keV is dominated by the K-40 Compton distribution. Hereby, it is not relevant whether the K-40-source is located in the counting source, in the detector materials or in the components of the shielding or whether it originates in background contributions from the surroundings of the spectrometer (e. g. in the walls of buildings). Therefore, a high peak-to-Compton ratio is particularly advantageous.

The HPGe detector described in the example below is proved to be suitable for a wide range of tasks:

— Crystal diameter: 65,5 mm;

— Crystal height: 60 mm;

— Relative efficiency (referring to a 3“ × 3“ NaI(Tl) crystal): 50 %;

— Full width at half maximum of the 1332,5 keV gamma peak of Co-60: 1,9 keV;

— Peak-to-Compton ratio: 60/1.

2.2 Shielding

Shielding the detector is fundamentally necessary to minimize the influence of ambient radiation. Several materials may be used for shielding: lead, steel, cadmium and copper or combinations of those. The shielding material itself should contain as few radioactive impurities (such as Pb-210 in lead, other natural radionuclides or Co-60 in steel components) as possible. The most frequently used shielding material is lead. Optimal shielding efficiency is achieved when the detector crystal is entirely surrounded by a lead housing with a thickness of 5 cm to 10 cm.

For low-level measurement systems, a lead thickness of 15 cm is sufficient to suppress the 1460,8 keV peak of K-40 (e. g. emitted by the walls of buildings). However, the lead used for this purpose must exhibit the lowest possible intrinsic Pb-210 activity. This is particularly relevant when determining low-level Pb-210 activities.

Gamma radiation, in particular emitted by the counting source, generates X-ray fluorescence radiation at approximately 75 keV originating from the lead shielding. To absorb this radiation, the inner parts of the shielding are coated with material of lower atomic number (e. g. a cadmium sheet of 1 mm thickness, a copper sheet of 3 mm thickness or a 3 mm copper sheet combined with a 3 mm Perspex sheet).

To reduce the influence of scattered radiation on the pulse height spectrum, the minimum distance between the shielding and the counting source and the detector, respectively, should be 10 cm. This distance also facilitates the handling of the counting sources inside the shielding.

Due to its radon content, the air remaining inside the shielding also contributes to the spectrum continuum via the radon progenies Pb-214 and Bi-214. Radon can be expelled from inside the shielding, for example, by flushing with nitrogen evaporating from the dewar via a hose system.

2.3 Electronic unit

The electronic unit consists of the following components:

— the high-voltage supply;

— the preamplifier;

— the main amplifier to form the pulses and amplify with an adjustable pulse shape time constant, integrated in or separate from

— the pulse height analyser consisting of an analogue-to-digital converter (ADC) and a storage unit.

Normally, the preamplifier is an integral part of the detector, since its input stage is also cooled. For low-level measurements, the preamplifier is usually placed outside the lead shielding in order to shield the detector from the electronic components' intrinsic activity. With this configuration, attention must be paid to ensure that the remaining ring slit between the cryostat and the lead shielding is as small as possible.

In addition, it is possible to use a pulse generator to verify the function of the electronic components and to correct for pile-up losses (see Section 9.3) that may occur in measurements at higher activities.

Essentially, there are three concepts for arranging and operating these components:

— the historical concept that consists of separate components for the high-voltage supply, the main amplifier, the ADC plug-in unit, the multichannel analyser, etc.;

— another historical concept, which is still in use in certain cases, based on a computer that is equipped with an ADC on a plug-in card and a software program to analyse the height of the pulses and compute the activity;

— the state-of-the-art concept where the power supply, the main amplifier, the ADC and the storage unit are integrated in one digital device. Some of these digital spectrometers can be integrated in common computer networks and operated by remote computers.

If an energy region from approx. 30 keV to approx. 2000 keV has to be covered, the pulse height analyser must have at least 4096 channels (see Section 5). Thus, the full width at half maximum of the 1332,5 keV gamma peak of Co-60 is described with the minimum required number of four channels for peak evaluation [2]. However, it is advantageous to have 8192 channels available, since the full width at half maximum corresponds to eight channels in this case.

2.4 Computer and evaluation software

A gamma spectrometric measurement system is usually equipped with a computer and a spectrometry software. This software allows to adjust and control the operating parameters of the gamma spectrometric detector, to control the measurement operation, and to evaluate the pulse height spectra.

To evaluate the pulse height spectra, the software should have at least the following functions:

— searching and evaluating peaks in the pulse height spectrum automatically and manually (see Section 5.1);

— determining the exact channel position of a peak (see Section 5.1);

— assigning the peaks to certain radionuclides by means of a radionuclide library (see Section 5.2);

— calculating the net pulse count N_{n} in a gamma peak and the standard uncertainty of N_{n} taking the peaks of the spectrum continuum into account (see Section 5.3), including a graphic representation;

— deconvolution of multiplets (see Section 5.4);

— evaluation of the energy calibration (see Section 6.1);

— calibrating the efficiency according to the specific nuclide and energy (see Section 6.3);

— considering the correction factors for coincidence summations (see Section 7 and Annex D) and self-attenuation (see Section 8), the correction of pile-up and dead-time effects (see Section 9.3) as well as the decay correction (see Section 9.4);

— considering interferences due to peaks of other radionuclides (see Section 9.6 and General Chapter γ-SPEKT/INTERF of this Procedures Manual);

— calculating the activities and the activity concentrations (see Sections 5.3, 9.1, 9.2, and 9.8);

— calculating specific activities (see Section 9.10 and Annexes A and B);

— determining the measurement uncertainty (see Section 9.11);

— determining the characteristic limits (see Section 10 and Annex C as well as the General Chapter ERK/NACHWEISGR-ISO-01 of this Procedures Manual);

— documenting the results in a measurement and evaluation protocol containing all the information on the data used (background, efficiency, radionuclide data, etc.) and stating the version number and the date of generation.

In addition, file management modules and quality assurance modules are also available.

3 Geometry of the counting sources

Depending on the amount at hand or the expected activity, the material to be measured is filled in test tubes, cans or bottles. Additionally, Marinelli beakers allow the counting source to be positioned laterally from the detector, which increases the detection sensitivity. Marinelli beakers are available both in single-use or in multiple-use design and with various inner diameters, which correspond to frequent outer diameters of detector end caps, and with various filling volumes (see Figure 2).

Fig. 2: Examples of common Marinelli beakers

The containers are placed either directly on the detector end cap or in a suitable source holder. In both cases, the position of the counting source must agree with the position of the calibration source. In addition, the containers used for calibration and for the measurement must have the same dimensions and identical filling heights. When measuring the activity in powdery or granulous materials, the formation of cones must be prevented, and the surface must be plane-parallel to the bottom of the measurement container. The form of the counting source may no longer be modified by tilting, shaking or stamping once the measurement container has been sealed, since this could compress the material to be measured and thus reduce the filling height of the measurement container.

With counting sources in the form of filter cakes, which are generated by radiochemical separation, it may be difficult to achieve identical measurement conditions to those prevailing with the calibration source. In the case of such counting sources, waviness of the filter cake may be remedied, for example, by applying a Perspex disk or a suitable tape. If the filter cake is subjected to further radiochemical processing steps after the gamma spectrometric measurement, the counting source may be fixed by means of a

small ring to weigh down the uncovered edge of the cake, for instance, in a measurement tray before drying the filter cake (see Figure 3).

Fig. 3: Filter cake fixed in the measurement tray by means of a retainer ring.

To prevent contamination, the detector end cap should be covered with a thin foil, such as cling film or a small household bin liner. To prevent the formation of condensation – and thus corrosion of the detector end cap – the foils must be regularly replaced.

4 Detection efficiencies for gamma-rays

The efficiency is defined as the ratio of the count rate (in s^{-1}) obtained at calibration, which is caused by radiation of a certain type and energy, to the known emission rate (in s^{-1}) of this type of radiation from the calibration source.

In gamma spectrometry, one differentiates between different efficiencies due to physical processes:

— full energy peak detection efficiency, which refers to the full energy peak;

— total detection efficiency, which is defined as the ratio of all counts registered in the spectrum to the number of emitted photons. This also includes counts from photons (see Section 5) that reach the detector after scattering processes have taken place in the measuring chamber.

These detection efficiencies are required to quantitatively evaluate the pulse height spectra. They are determined either by measurement or by means of mathematical procedures (see Section 6.3).

5 Evaluating the pulse height spectrum

Gamma rays interact with the detector crystal. These interactions are known as photo effect, Compton effect and electron pair production and generate electric voltage pulses. The pulse height analyser assigns these as counts to the channels of the multichannel analyser proportionally to the energy deposited in the detector crystal. The duration of measurement used to evaluate the pulse height spectrum is the live time (see Section 9.3).

The distribution of the frequency of occurrence of the counts registered in the channels during the duration of measurement is called pulse height spectrum and may be very complex. It includes both broad distributions and narrow peaks. The quantitative evaluation is solely based on the peaks as they represent the entire gamma energy due to the photo effect. Such peaks are called full energy peaks. The radionuclides contained in the counting source are identified based on the position of the gamma peaks in the pulse height spectrum, which provide the information on the energy. For this purpose, a radionuclide library (see Section 5.2) and a calibration of the gamma spectrometric measurement system (see Section 6) are necessary.

The activity of a radionuclide is proportional to the net count rate in the gamma peak considered. By subtracting the inevitable background contribution from the gross count rate, the net count rate is determined.

5.1 Peak search

Automatic or manual peak search procedures of the gamma spectrum evaluation software are used [3, 6].

The sensitivity for the detection of peaks when using the automatic peak search is controlled by means of adjustable parameters. If the sensitivity is set too low, only the prominent peaks (i. e. those that are clearly higher than the spectrum continuum) are detected. If the sensitivity is too high, even peaks that are merely due to statistical variations in the spectrum continuum are detected. The sensitivity must, therefore, be adjusted as accurately as possible for the measurement task at hand.

In addition to the evaluation of the pulse height spectrum, it also allows a peak evaluation at the regions of interest (ROIs) in the pulse height spectrum to be obtained for all peak entries available in the radionuclide library.

Combining both procedures is recommended. More intensive peaks are found by means of the automatic search. Peaks with low count numbers or peaks that are "hidden" in the tailings of a peak with numerous counts can be identified with the aid of the library-oriented search.

5.2 Radionuclide library

The radionuclide library is a collection of radionuclide-specific data that are necessary to be able to assign gamma peaks to radionuclides and to determine their activity. Gamma spectrometric software programs usually contain an exhaustive radionuclide library which the user can call upon to create his/her own customized libraries. The library contained in the software already contains a large number of radionuclides (among other values and uncertainties of half-lives, energies and emission intensities).

The radionuclide data must be kept up-to-date (see General Chapter KERNDATEN of this Procedures Manual), which implies accurate documentation, data management and data backup.

In practice, often a master library is created containing the nuclear data relevant to all the radionuclides that are relevant to the user's measurement tasks. The specific libraries (e. g. for special types of detectors, sample materials, measurement geometries, parent-progeny relations) are then generated based on this master library.

Note:

— With parent-progeny relations, particular attention must be paid to replacing the half-life of a short-lived progeny nuclide by the half-life of a long-lived parent nuclide, so that no physically absurd activities are calculated when correcting the decay to a reference point in time of an environmental sample which lies a longer period of time before the time of measurement.

— When measuring natural radionuclides, it is advantageous to create radionuclide libraries that are optimized for radioactive equilibrium or for radioactive disequilibrium (see Annex E and the General Chapter γ-SPEKT/NATRAD of this Procedures Manual).

— In addition, attention must also be paid to pure summation peaks. These are peaks that occur in particular in special geometries (e. g. measurements in borehole detectors) as the sum of two or more gamma or X-ray photons. If the energies of these two (or more) photons is registered at the same time by the detector, the peaks thus generated in the spectrum are most of the time not part of the radionuclide libraries.

To detect multi-line radionuclides in one pulse height spectrum, their relevant peaks must be selected in the radionuclide library used.

Moreover, the radionuclide library contains the emission intensities of gamma-ray or X-ray photons that are required to calculate the activity of the radionuclides detected in the counting source (see Section 9). Hereby, coincidence summation effects and self-absorption effects (see Sections 7 and 8) must be taken into account. For this purpose, certain software packages allow the user to add experimentally determined correction factors to the radionuclide library.

5.3 Count number under an undisturbed gamma peak (singlet)

To calculate the activity of a radionuclide, the net count number in the gamma peak is required.

In the following, three frequently used procedures will be presented:

— the summation procedure (see Section 5.3.1.);

— the empirical step function procedure (see Section 5.3.2), and

— the peak fitting procedure (see Section 5.3.3).

5.3.1 Summation procedure

This is the easiest of all procedures. Its first step is the determination of the gross count number in a gamma peak by summing up the count numbers in the different channels of the energy region considered. Then, the net count number is obtained by subtracting the count number of the contributions of the spectrum continuum and of possibly occurring background contributions from the peak to be evaluated according to Equation (3).

Note:
The contributions of the spectrum continuum consist mainly of the Compton scattering of photons originating from the sample or from the counting source or from the environment and of external contributions such as electronic disturbances.

A sketch of this procedure is shown in Figure 4 in which the grey area is called region of interest (ROI). This region of interest consists of the peak base width b and of the channel ranges L_d and L_s for determining the spectrum continuum.

The peak base width b is either defined manually by markings on the screen or selected automatically by the program. b is usually stated as multiples of the full width at half maximum h, e. g. $b = 2{,}5 \cdot h$ (see Figure 6).

The contribution of the spectrum continuum in the area of the gamma peak considered is calculated by means of the so-called trapeze procedure. For this purpose, the sums of the count numbers N_d and N_s, respectively, in the channel ranges L_d and L_s, respectively, are determined (see Figure 4). The channel ranges L_d and L_s are usually selected so as to have the same width; in the case of complex spectra, they may, however, be selected in such a way that they have different widths.

From the count numbers per channel N_K and the duration of measurement t_m, it is possible to calculate the gross count rate R_g, the trapezoidal continuum background count rate $R_\mathrm{T,}$ and the net count rate R_n. For this purpose, K_1 is used for the left edge channel and K_2 for the right edge channel with the peak base width b in the equations below.

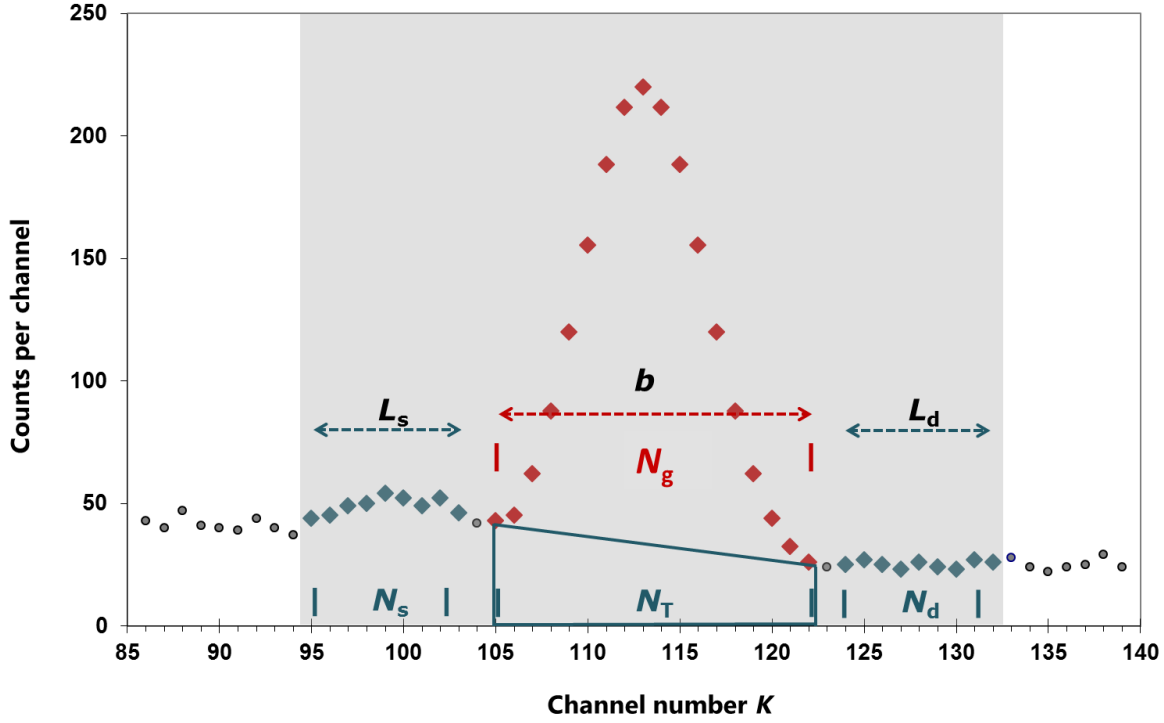

Tab. 1: Quantities to be taken into account in the ROI (shaded in grey) when using the summation procedure, with

N_g gross count number in the peak;
N_T trapezoidal continuum background count number in the peak;
N_s sum of the count numbers in the channel range L_s;
N_d sum of the count numbers in the channel range L_d.

$$R_g = \frac{N_g}{t_m} = \frac{1}{t_m} \cdot \sum_{K=K_1}^{K_2} N_K \tag{1}$$

$$R_T = \frac{N_T}{t_m} = \frac{1}{t_m} \cdot \frac{b}{2} \cdot \left(\frac{N_s}{L_s} + \frac{N_d}{L_d}\right) = \frac{1}{t_m} \cdot \frac{b}{2} \cdot (\bar{N}_s + \bar{N}_d) \tag{2}$$

$$R_n = R_g - R_T - \left(R_{0,g} - R_{0,T}\right) \tag{3}$$

The standard uncertainties of the individual count rates are calculated according to Equations (4) to (6).

$$u(R_g) = \sqrt{\frac{R_g}{t_m}} \tag{4}$$

$$u(R_T) = \sqrt{\frac{R_T \cdot b}{2 \cdot \bar{L} \cdot t_m}} \tag{5}$$

$$u(R_\mathrm{n}) = \sqrt{u^2(R_\mathrm{g}) + u^2(R_\mathrm{T}) + u^2(R_{0,\mathrm{g}}) + u^2(R_{0,\mathrm{T}})} = \\ = \sqrt{\frac{R_\mathrm{g}}{t_\mathrm{m}} + \frac{R_\mathrm{T} \cdot b}{2 \cdot \bar{L} \cdot t_\mathrm{m}} + \left(\frac{R_{0,\mathrm{g}}}{t_0} + \frac{R_{0,\mathrm{T}} \cdot b_0}{2 \cdot \bar{L}_0 \cdot t_0}\right)} \qquad (6)$$

where $$\bar{L} = \frac{\bar{N}_\mathrm{s} + \bar{N}_\mathrm{d}}{\frac{\bar{N}_\mathrm{s}}{L_\mathrm{s}} + \frac{\bar{N}_\mathrm{d}}{L_\mathrm{d}}}$$

Herein are:

$R_{0,\mathrm{g}}$ gross count rate of the gamma peak considered in the background spectrum, in s^{-1};

$R_{0,\mathrm{T}}$ trapezoidal background gross count rate of the gamma peak considered in a separate background spectrum, in s^{-1};

$\bar{L}, \bar{L}_0$ average channel range on either side of the gamma peak considered: if $L_\mathrm{s} = L_\mathrm{d} = L$, then $\bar{L} = L$ applies.

5.3.2 Empirical step function procedure

Another method to determine the net count number in the gamma peak considered is the empirical step function procedure. In this procedure, a step function $S_\mathrm{e}(K)$ is used instead of the trapeze described in the summation procedure to determine the contribution of the spectrum continuum under the gamma peak considered.

In Equation (7), the step function $S_\mathrm{e}(K)$ is described by means of the average count numbers $N_\mathrm{s}/L_\mathrm{s}$ and $N_\mathrm{d}/L_\mathrm{d}$ (see Figure 5).

$$S_\mathrm{e}(K) = \frac{N_\mathrm{d}}{L_\mathrm{d}} + \left(\frac{N_\mathrm{s}}{L_\mathrm{s}} - \frac{N_\mathrm{d}}{L_\mathrm{d}}\right) \cdot \frac{S_1(K)}{S_2} = \bar{N}_\mathrm{d} + (\bar{N}_\mathrm{s} - \bar{N}_\mathrm{d}) \cdot \frac{S_1(K)}{S_2} \quad \text{with} \quad K_1 < K < K_2 \qquad (7)$$

with the auxiliary quantities:

$$S_1(K) = \sum_{m=K}^{K_2} N_m \qquad \text{and} \qquad S_2 = S_1(K = K_1) = \sum_{m=K_1}^{K_2} N_m = N_\mathrm{g} \qquad (8)$$

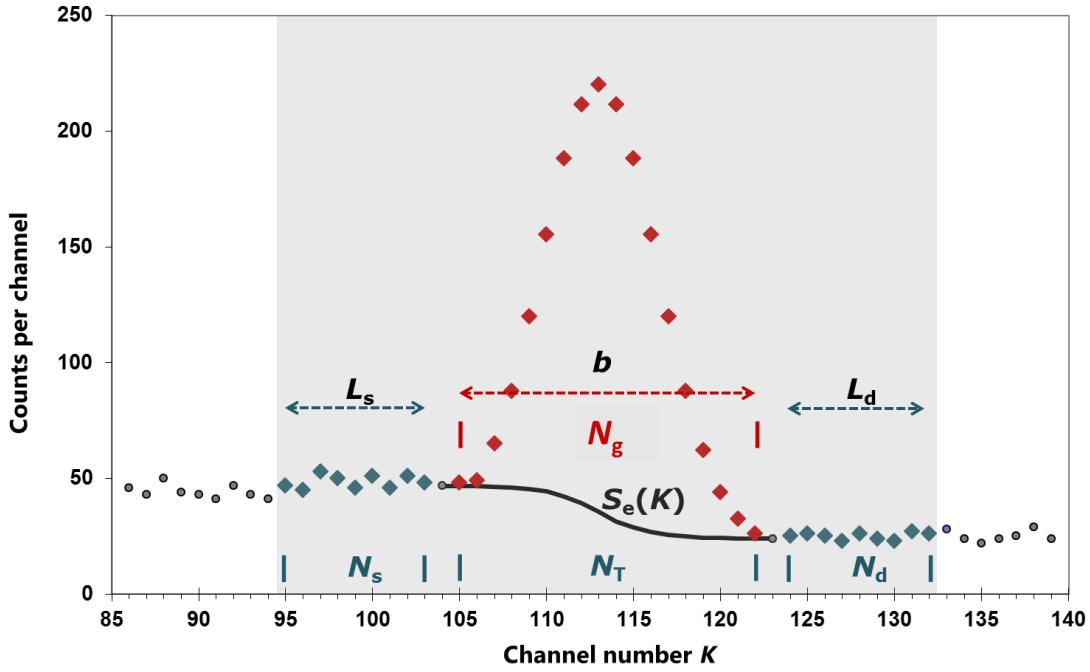

Fig. 4: Schematic representation of the empirical step function $S_e(K)$ for a gamma peak

The trapezoidal continuum background count rate R_T results from the summation channel per channel of the function values across the range of the peak base width $b = K_2 - K_1 + 1$.

$$R_T = \frac{1}{t_m} \cdot \left[b \cdot \bar{N}_d + (\bar{N}_s - \bar{N}_d) \cdot \frac{\sum_{K=K_1}^{K_2} S_1(K)}{S_2} \right] \tag{9}$$

where

$$\sum_{K=K_1}^{K_2} S_1(K) = \sum_{K=K_1}^{K_2} \sum_{m=K_1}^{K_2} N_m \tag{10}$$

The net count rate R_n is calculated according to Equation (11):

$$R_n = R_g - R_T - (R_{0,g} - R_{0,T}) = \frac{N_g}{t_m} - \frac{N_T}{t_m} - \left(\frac{N_{0,g}}{t_0} - \frac{N_{0,T}}{t_0} \right) \tag{11}$$

The uncertainties of the trapezoidal continuum background count rate R_T and of the net count rate R_n are calculated by means of Equations (12) and (13).

$$u^2(R_T) = \frac{1}{t_m^2} \cdot \frac{\bar{N}_s}{L_s} \cdot \left(\frac{\sum_{K=K_1}^{K_2} S_1(K)}{S_2} \right)^2 + \frac{\bar{N}_d}{L_d} \cdot \left(b - \frac{\sum_{K=K_1}^{K_2} S_1(K)}{S_2} \right)^2 \tag{12}$$

$$u(R_{\mathrm{n}}) = \sqrt{\frac{R_{\mathrm{g}}}{t_{\mathrm{m}}} + u^2(R_{\mathrm{T}}) + \frac{R_{0,\mathrm{g}}}{t_0} + u^2\left(R_{0,\mathrm{T}}\right)} \tag{13}$$

5.3.3 Peak fitting procedure

The peak fitting procedure allows the net pulse number of a singlet gamma peak to be calculated directly by fitting a summation function f_{Sg} consisting of several components to the pulse height spectrum in the ROI, as described in Equation (14).

$$f_{\mathrm{Sg}} = U(K) + S_{\mathrm{f}}(K) + G(K) + T(K) \tag{14}$$

Hereby, the basic shape of the gamma peak is described by means of the Gaussian function $G(K)$, whereas deviations from its ideal shape are described by the tailing function $T(K)$. The spectrum continuum that must be taken into account consists of a spectrum continuum polynomial $U(K)$ and a step function $S_{\mathrm{f}}(K)$, as shown in Figure 6 and Figure 7.

The summation function is fitted to the pulse height spectrum by means of the non-linear weighted least-squares method. Starting values are set for the parameter k_0, N_{n}, σ and σ_{T}, which are required for this purpose. These values will then be optimized within the course of the calculations; the starting values for σ and σ_{T} are, however, taken from the calibration of the peak shape (see Section 6.2).

Note:
When evaluating peaks with low count numbers, it may be helpful to keep the starting values for k_0, σ and σ_{T} constant to progressively transform the non-linear fitting procedure into a linear one.

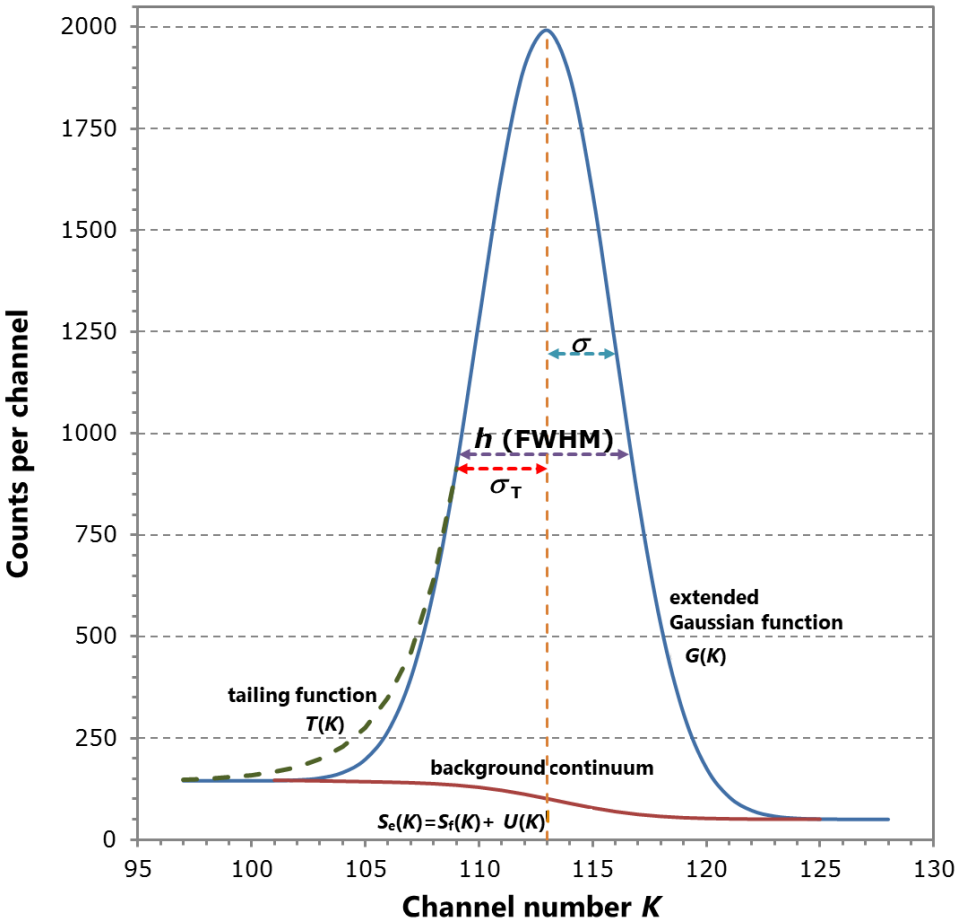

Fig. 5: Schematic representation of the components of the summation function f_{Sg} during the peak fitting.
From channel 109 (red double arrow) down, the Gaussian function progressively becomes a tailing function. In addition, the full width at half maximum h (FWHM), the width parameter σ of the Gaussian function, and the tailing parameter σ_{T} are represented.

5.3.3.1 Gaussian function $G(K)$

The Gaussian function to be fitted $G(K)$ is calculated according to Equation (15).

$$G(K) = N_{\mathrm{n}} \cdot \frac{1}{\sigma \cdot \sqrt{2 \cdot \pi}} \cdot \mathrm{e}^{-\frac{(K-k_0)^2}{2 \cdot \sigma^2}} \tag{15}$$

where

K channel number;

k_0 centre of the peak in relation to the channel numbers (it does not necessarily have to be an integer);

N_{n} net count number in the peak;

σ width parameter of the Gaussian function in channels.

Note:

— The factor before the exponential function in Equation (15) represents the amplitude of the gamma peak.

— The relation between the width parameter σ and the full width at half maximum h of a gamma peak is: $h = 2{,}355 \cdot \sigma$.

— The full width at half maximum of the gamma peak should not be smaller than four channels.

— The ratio of the step height to the amplitude of the gamma peak (see Figure 6) depends on the energy; in addition, it also depends on the material of the counting source, its density and its filling height. In the medium energy region between approx. 100 keV and 1500 keV, the step height is relatively constant. At lower and higher energies, it increases unequally. For information about the effects contributing to the step height, please refer to [7].

5.3.3.2 Tailing function $T(K)$

The so-called tailing is a detector property that leads to the left slope of the gamma peak being slightly higher than the ideal Gaussian function. To describe this tailing fraction, the Gaussian function $G(K)$, for example at the point $K = k_0 - \sigma_T$, increases constantly to eventually become an exponential function $T(K)$. This effect is described in Equation (16), where σ_T is designated as the tailing parameter (see Figure 6).

$$T(K) = N_n \cdot \frac{1}{\sigma \cdot \sqrt{2 \cdot \pi}} \cdot e^{-\frac{\sigma_T^2}{2 \cdot \sigma^2} + \sigma_T \cdot \frac{K - k_0}{\sigma^2}} \tag{16}$$

The smaller the value of the ratio σ_T to h, the greater the tailing effect. As soon as the ratio of σ_T to h equals 1, the contribution of tailing becomes negligible. Taking the tailing effect into account modifies the net area. Its new value $N_{n,T}$ is described by means of the following relation:

$$N_{n,T} = N_n \cdot \left(\Phi \cdot \frac{\sigma_T}{\sigma} + \frac{1}{\sqrt{2 \cdot \pi}} \cdot \frac{\sigma}{\sigma_T} \cdot e^{-\frac{\sigma_T^2}{2 \cdot \sigma^2}} \right) \tag{17}$$

5.3.3.3 Spectrum continuum

The spectrum continuum consists of a spectrum continuum polynomial $U(K)$ and a step function $S_f(K)$. In the case of small peak areas, the polynomial of the spectrum continuum $U(K)$, which is described by means of a linear or square function of the channel number, is the determining fraction of the spectrum continuum. With increasing peak area, the fraction of the step function $S_f(K)$ in the spectrum continuum prevails.

$$S_f(K, k_0) = \frac{N_n}{\sqrt{2 \cdot \pi \cdot \sigma^2}} \cdot \frac{s_{rel}}{1 + e^{\frac{K - k_0}{\sigma}}} \tag{18}$$

In Equation (18), s_{rel} means the ratio of the step amplitude to the amplitude of the gamma peak. This ratio is constant and independent of the current activity.

Note:

If the area under the gamma peak is zero, the spectrum continuum only consists of the contribution of the polynomial of the spectrum continuum $U(K)$. The decision threshold is determined based on this area (see Section 10).

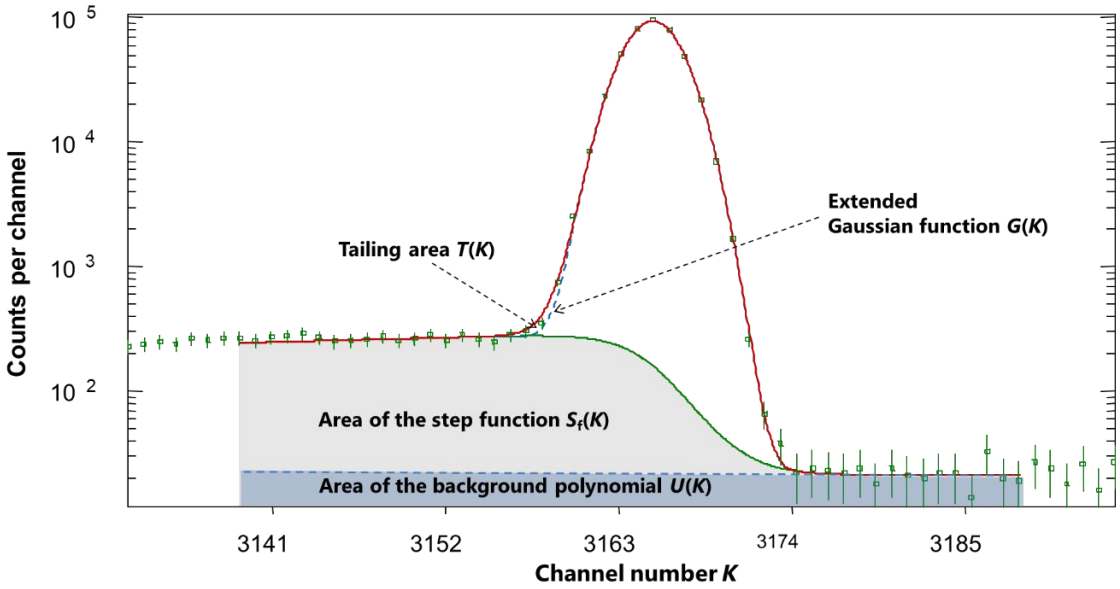

Fig. 6: Schematic representation of the spectrum continuum, which consists of the area under the step function $S_{\mathrm{f}}(K)$ and the polynomial of the spectrum continuum $U(K)$.

5.4 Count number under a group of gamma peaks (multiplet)

A group of gamma peaks that lie close to each other or overlap is called a multiplet. These gamma peaks can belong either to one or several radionuclides.

Before calculating the activities of the radionuclides involved, the multiplets must be separated, and the areas thus obtained must be assigned to each of the radionuclides. In the easiest case, in which two gamma peaks only slightly overlap, the multiplet can be separated in the minimum between the two gamma peaks. In all other cases, the summation function f_{Sg} of the peak fitting procedure (see Section 5.3.3) is extended to the number n of existing peaks to obtain the summation function of the multiplet f_{Mp}.

$$f_{\mathrm{Mp}}(K,k_{0,i}) = U(K) + \sum_{i=1}^{n}\left[S_{\mathrm{f}}(K,k_{0,i}) + G(K,k_{0,i}) + T(K,k_{0,i})\right] \tag{19}$$

The net count numbers $N_{\mathrm{n},i}$ to be determined for each of the individual gamma peaks of the multiplet are included as factors in the functions $S_{\mathrm{f}}(K,k_{0,i})$, $G(K,k_{0,i})$, and $T(K,k_{0,i})$ (see Section 5.3.3).

6 Calibration of a gamma spectrometric measurement system

A gamma spectrometric measurement system must be calibrated to determine the specific activity and the specific concentration, respectively, of radionuclides by means of the net count numbers N_n or net count rates R_n determined when evaluating the pulse height spectra. The calibration steps required for this purpose are described below in more detail.

6.1 Energy calibration

The energy calibration establishes the relation between the channel number of the pulse height spectrum and the energy of the photon radiation in accordance with Equation (20). The occurring polynomial coefficients e_0, e_1, and e_2 are determined by calibration.

$$E_j = e_0 + e_1 \cdot K_j + e_2 \cdot K_j^2 \tag{20}$$

For this purpose, one or several calibration sources with known gamma-emitting radionuclides are used by means of which the corresponding channel number K_j of the peak maximum is determined for the respective photon energy E_j. The more calibration points are available, the more accurate the energy calibration becomes.

Prior to calibration, the electronic components of the gamma spectrometric measurement system must be adjusted to the energy region which depends on the measurement at hand (see Section 2.3). For an energy range from 0 keV to 2000 keV at 4096 channels, for example, one has to check whether the boundary conditions E_j (K_j = 0) = e_0 ≈ 0 keV and E_j (K_j = 4096) ≈ 2000 keV apply. A significant deviation from these values requires a readjustment of the electronic components.

Note:

The polynomial coefficient e_2 should have a value less than 10^{-7} keV · (channel)$^{-2}$; if this is not achieved, the measurement system must be readjusted.

In order to identify radionuclides with certainty, the standard uncertainty of energy-related position requires to be lower than the full width at half maximum h of the gamma peak considered.

Within the scope of quality assurance, the energy calibration must be checked at regular intervals (see also General Chapter QUAKO/INTERN of this Procedures Manual).

6.2 Calibration of the energy dependence of the peak shape

The full width at half maximum h is used for peak searching, for determining the count number and for identifying the radionuclides; it must therefore be calibrated as a function of the energy (see Figure 8). For this purpose, individual peaks with a high count number are used that are distributed across the entire energy region.

In particular when using the peak fitting procedure in accordance with Section 5.3.3, it is indispensable to know the energy dependence of the peak shape, since the starting values for the parameters σ and σ_T have to be optimized and the amplitude of the step function $S(K)$ are derived from it. Hereby, the relation $h = 2{,}355 \cdot \sigma$ applies.

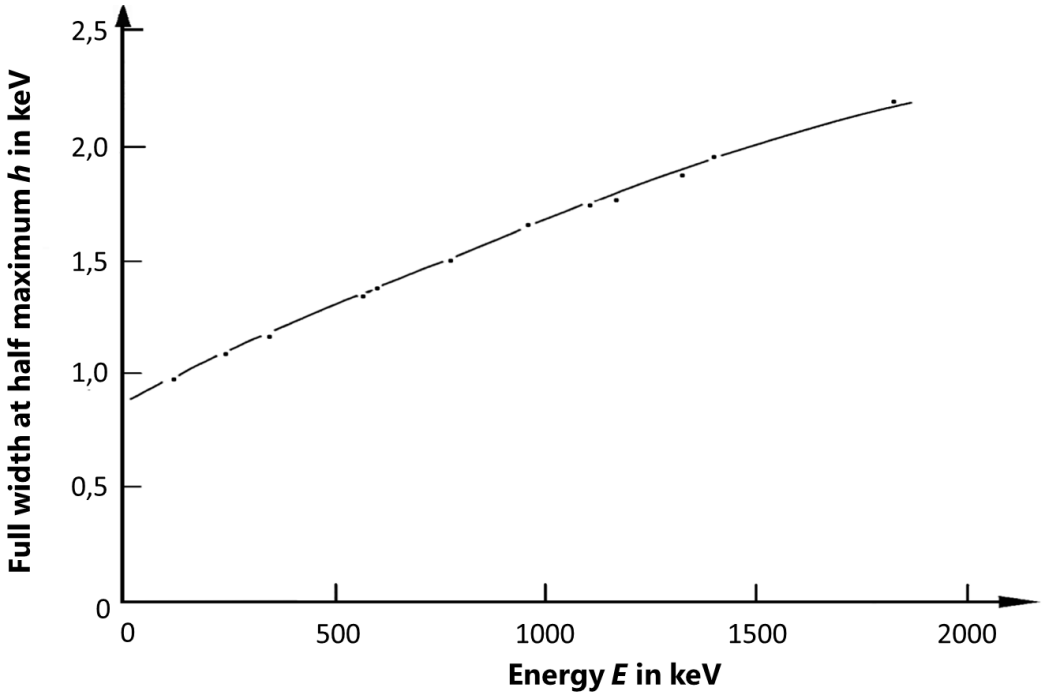

Fig. 7: Example of the dependence of the full width at half maximum h on the energy E

Equation (21) is used to describe the full width at half maximum h as a function of the gamma-ray energy E:

$$h(E) = \sqrt{a + b \cdot E} \tag{21}$$

The parameters a and b are determined analogically to the polynomial coefficients of the energy calibration.

The remaining energy-dependent peak shape parameters – the tailing parameter σ_T and the amplitude of the step function – are usually determined by means of internal algorithms of the evaluation software.

6.3 Determining the detection efficiency

The detection efficiency has to be determined on the one hand for a specific nuclide (see Section 6.3.1) and on the other hand as a function of the energy (see Section 6.3.2). Depending on the measurement task, one of those two calibration types is necessary to obtain the quantitative relation between the net count rate R_{n} of a gamma peak in the pulse height spectrum and the activity prevailing in the counting source. For this purpose, calibration sources of known activity and nuclide composition are required.

As an alternative, the detection efficiency may be determined by means of mathematical procedures (see Section 6.3.3).

Calibration sources are available in the form of aqueous solutions, gels or synthetic resins among others. The geometry and the matrix of calibration sources and sources to be measured should be, as far as possible, in agreement to minimize the need for corrections.

Note:
As a replacement for aqueous solutions, synthetic resin calibration sources are available. These sources may contain additives to reach a density of 1,0 g·cm^{-3}. These additives have different atomic numbers from the atoms in the water molecule and therefore influence the efficiency, especially at gamma-ray energies below 100 keV.

The radionuclide composition of the calibration sources must be geared to the measurement task at hand. Hereby, the calibration sources should exhibit activities that keep the dead time and the pile-up effects as small as possible (see Section 9.3), are traceable to a national primary standard, and whose relative standard uncertainties are around 1 % to 2 %.

When carrying out the calibration measurements, the duration of measurement must be selected in such a way that the values of the relative standard uncertainties of the individual gamma peaks' net count rates are around 1 % to 2 %.

6.3.1 Nuclide-specific calibration

The nuclide-specific calibration is the simplest type of calibration. The detection efficiency, ε_{r}, for a radionuclide r, thus determined, is only valid under the following conditions:

— The calibration sources must contain the radionuclides to be determined in the counting source.

— The composition and the density of the sources should be similar.

— The measurement geometries of the calibration sources and of the counting sources must be identical (see Section 3).

The detection efficiency ε_{r} for a radionuclide r is calculated as the quotient of the net count rate R_{n} and of the activity A according to Equation (22).

$$\varepsilon_{\mathrm{r}} = \frac{R_{\mathrm{n}}}{A} \tag{22}$$

In the case of radionuclides with several emission peaks, Equation (22) applies to each individual emission peak accordingly. It is not necessary to correct the coincidence summation. The reciprocal $\varphi_{\mathrm{A}} = A/R_{\mathrm{n}}$ is also called the calibration factor.

6.3.2 Calibration as a function of the energy

For measurement tasks in which unknown radionuclide compositions occur, the evaluation of the pulse height spectrum requires the efficiency as a function of the energy.

Two procedures are available to calibrate the efficiency. They are explained below.

6.3.2.1 Calibration as a function of the energy with single-line radionuclides

A calibration source is used containing a sufficient activity of any number of gamma-emitting radionuclides with only one emission peak in the energy region between 100 keV to 1200 keV, e. g. Mn-54, Zn-65, Sr-85 or Cs-137. A second calibration source is used to extend the calibration curve to energies below 100 keV. This calibration source contains nuclides such as Co-57, Cd-109, Pb-210 and Am-241.

For the high-energy region, natural radioactive K-40 is available. Its use necessitates long durations of measurement to reach the required standard uncertainty for this calibration point.

Note:
Instead of K-40, it is possible to use the multi-line radionuclide Y-88 whose use, however, requires coincidence summation corrections, as described in Section 6.3.2.2.

The efficiency $\varepsilon(E_i)$ in $\mathrm{Bq^{-1}{\cdot}s^{-1}}$ is calculated according to Equation (23) for each emission peak measured.

$$\varepsilon(E_i) = \frac{R_{\mathrm{n}}(E_i)}{A_{\mathrm{r}} \cdot p_{\gamma,\mathrm{r}}(E_i)} \tag{23}$$

where

$R_{\mathrm{n}}(E_i)$ net count rate of the peak at the energy E_i, in $\mathrm{s^{-1}}$;
$p_{\gamma,\mathrm{r}}(E_i)$ emission intensity of the gamma peak of the radionuclide r at the energy E_i;
A_{r} activity of the radionuclide r, in Bq.

A calibration curve is fitted to the calculated efficiencies, according to Section 6.3.2.3.

6.3.2.2 Calibration as a function of the energy with multi-line radionuclides

Multi-line radionuclides are radionuclides that emit photons with different gamma-ray energies. Typical multi-line radionuclides are radionuclides such as Co-60, Y-88, Ba-133, Cs-134, Eu-152 and Eu-154.

For calibration, radionuclides whose gamma peaks do not overlap and cover the desired energy region are preferable.

Note:
It is, in principle, possible to combine single-line and multi-line radionuclides to generate the calibration curve. Calibration sources with suitable radionuclide mixtures are commercially available.

The efficiency $\varepsilon(E_i)$ in $Bq^{-1} \cdot s^{-1}$ is calculated according to Equation (24) for each emission peak measured. Hereby, corrections for the coincidence summations in accordance with Section 7.2 must be taken into account.

$$\varepsilon(E_i) = \frac{R_{\mathrm{n}}(E_i)}{A_{\mathrm{r}} \cdot p_{\gamma,\mathrm{r}}(E_i)} \tag{24}$$

with

$f_{1,\mathrm{n},i}$ correction factor for the coincidence summation for the gamma peak i and the radionuclide r.

A calibration curve is fitted to the calculated efficiencies, in accordance with Section 6.3.2.3.

6.3.2.3 Calibration curve for the detection efficiency

A calibration curve is determined from the detection efficiencies $\varepsilon(E_i)$ calculated in accordance with Section 6.3.2.1 or Section 6.3.2.2.

Figure 9 shows examples of the energy dependence of the efficiency of different detector types. Depending on the type of detector, the efficiencies differ in the different energy regions, but the basic form of the curves remains comparable.

Such a curve can be divided into a low-energy region and a high-energy region and described with different function [2]. The curves of the two energy regions must merge in one point at the energy E_0, continually and with the same slope. The energy E_0 is specific to the detector and usually is comprised between 50 keV and 200 keV for Ge detectors.

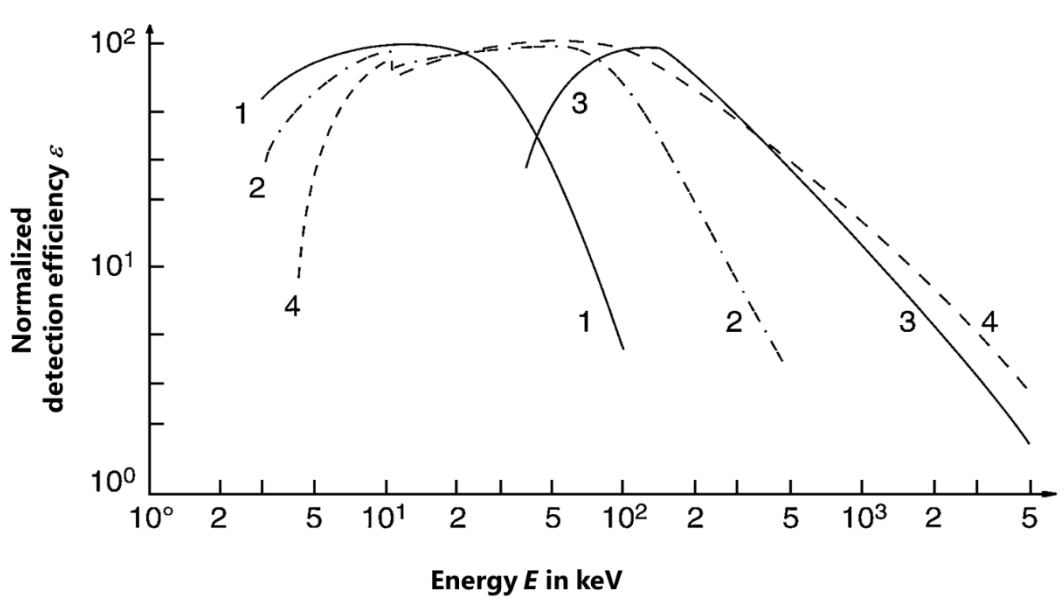

Fig. 8: Typical curve of the detection efficiency ε of different detectors as a function of the energy, determined with point-like sources, and standardization of the maximum of each curve to 100 %, in accordance with [2]:
1 Si(Li) detector;
2 planar p-type Ge detector (with K edge absorption at 10 keV);
3 coaxial p-type Ge detector;
4 coaxial n-type Ge detector

The functions below and above the energy E_0 are described by the Equations (25) and (26) according to [8]:

$$\ln \varepsilon(E) = v_1 + v_2 \cdot \ln\left(\frac{E}{E_0}\right) + v_3 \cdot \left[\ln\left(\frac{E}{E_0}\right)\right]^2 \qquad \text{for} \quad E \leq E_0 \tag{25}$$

$$\ln \varepsilon(E) = w_1 + w_2 \cdot \ln\left(\frac{E}{E_0}\right) + w_3 \cdot \left[\ln\left(\frac{E}{E_0}\right)\right]^2 \qquad \text{for} \quad E \geq E_0 \tag{26}$$

In order to meet the conditions of continuity and same slope at the energy E_0, the following must apply to the fitting parameters v_1:

$$v_1 = w_1 \qquad \text{and} \qquad v_2 = w_2$$

The entire curve can thus be described by means of Equation (27):

$$\ln \varepsilon(E) = v_1 + v_2 \cdot \ln\left(\frac{E}{E_0}\right) + v_x \cdot \left[\ln\left(\frac{E}{E_0}\right)\right]^2 \tag{27}$$

where

$$v_x = v_3 \qquad \text{for} \qquad E \leq E_0$$

$$v_x = w_3 \qquad \text{for} \qquad E \geq E_0$$

Besides the combinations of the two functions described above, commercial software provides further curve-fitting functions.

The standard uncertainty $u\big(\varepsilon(E)\big)$ of any random point on the fitted calibration curve at the energy E is estimated based on the fitting parameters v_i and their covariance matrix according to Equation (28):

$$u^2\big(\varepsilon(E)\big) = \sum_{i=1}^{m}\left(\frac{\partial\varepsilon(E)}{\partial v_i}\right)^2 \cdot u^2(v_i) + 2\sum_{i=1}^{m-1}\sum_{j=i+1}^{m}\left(\frac{\partial\varepsilon(E)}{\partial v_i}\right)\cdot\left(\frac{\partial\varepsilon(E)}{\partial v_j}\right)\cdot u\big(v_i, v_j\big) \qquad (28)$$

where

m number of fitting parameters.

6.3.3 Determining the detection efficiency mathematically

As an alternative to the procedures described in Sections 6.3.1 and 6.3.2 to determine the detection efficiency, these may also be determined mathematically.

For this purpose, so-called Monte Carlo (MC) methods are used to simulate the interactions of the photons with the measurement system. To this end, the geometric properties of the detector, including the properties of the crystal, must be known with sufficient accuracy. Since this is not always the case, the detection efficiency is determined mathematically by means of a combination of conventional calibration with a calibration source and an MC simulation. The results of such a determination must be validated with regard to their utilization and be traceable to a national primary standard.

The advantage of a mathematical determination is that the detection efficiencies can be calibrated for any kind of source, in nearly any geometry and basically for any sample material.

6.3.3.1 Fundamentals

In the following, a simplified example is described for calculating the full energy peak efficiency, which is based on a coaxial arrangement of the counting source and of the detector (see Figure 10).

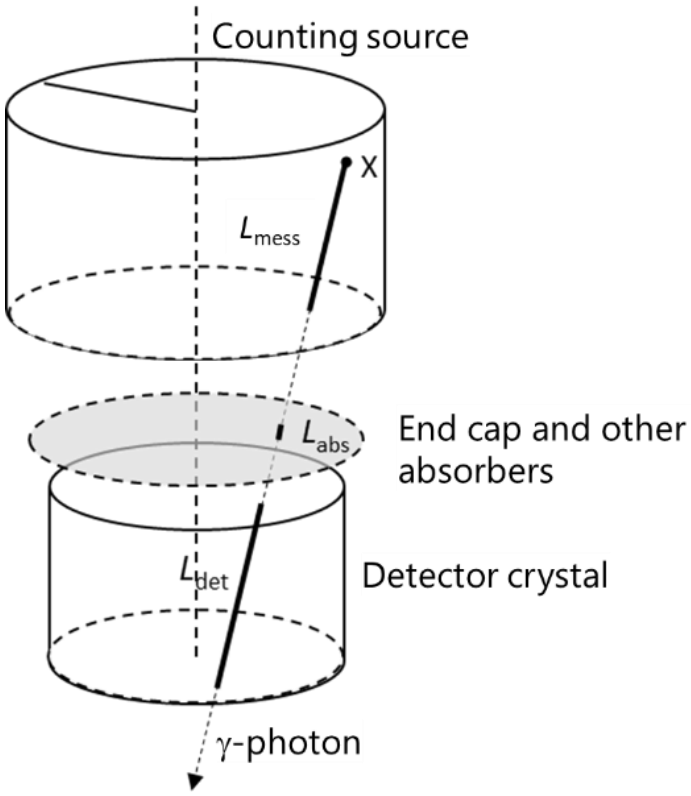

Fig. 9: Example of counting source and detector arrangement

A gamma photon, which is emitted at a point X inside the counting source towards the detector, leaves the counting source with the probability $p_{\mathrm{mess}}(L_{\mathrm{mess}})$ without energy loss due to absorption or scattering. If it hits the detector crystal, it will be detected there by a photoelectric interaction with the probability $p_{\mathrm{det}}(L_{\mathrm{det}})$.

$$p_{\mathrm{mess}}(L_{\mathrm{mess}}) = \mathrm{e}^{-\mu_{\mathrm{s,mess}} \cdot L_{\mathrm{mess}}} \tag{29}$$

$$p_{\mathrm{abs}}(L_{\mathrm{abs}}) = \prod_{j} \mathrm{e}^{-\mu_{\mathrm{s,abs}} \cdot L_{\mathrm{abs}}} \tag{30}$$

$$p_{\mathrm{det}}(L_{\mathrm{det}}) = 1 - \mathrm{e}^{-\mu_{\mathrm{s,det}} \cdot L_{\mathrm{det}}} \tag{31}$$

where

$\mu_{\mathrm{s,mess}}$ linear attenuation coefficient of the material of the counting source, in cm^{-1};

L_{mess} distance travelled by the gamma photon in the counting source, in cm;

$\mu_{\mathrm{s,abs}}$ linear attenuation coefficient of absorber materials, e. g. the end cap, in cm^{-1};

L_{abs} distance travelled by the gamma photon in the absorber material, in cm;

$\mu_{\mathrm{s,det}}$ linear attenuation coefficient of the detector due to the photoelectric effect, in cm^{-1};

L_{det} distance travelled by the gamma photon in the detector crystal, in cm.

The solid angle Ω is yielded by integration across all possible emission directions from which photons may reach the detector starting from a point X. By weighting with the product of the probabilities yielded by the Equations (29) to (31) and by considering the total volume of the counting source V_{P}, the so-called average effective solid angle $\bar{\Omega}_{\mathrm{P}}$ is obtained.

For the total geometric measurement arrangement, the calculation of $\bar{\Omega}_{\mathrm{P}}$ is done according to Equation (32):

$$\bar{\Omega}_{\mathrm{P}} = \frac{1}{V_{\mathrm{P}}} \cdot \int_{V_{\mathrm{P}}} \frac{1}{4 \cdot \pi} \int_{\Omega_{\mathrm{det}}} \left[p_{\mathrm{mess}}(L_{\mathrm{mess}}, \dots) \cdot \prod_{j} p_{\mathrm{abs}}(L_{\mathrm{abs}}, \dots) \cdot p_{\mathrm{det}}(L_{\mathrm{det}}, \dots) \right] \mathrm{d}\Omega_{\mathrm{P}}\, \mathrm{d}V_{\mathrm{P}} \tag{32}$$

This is the basis for the mathematical approach to the detection efficiency transfer described in Section 6.3.3.3.

6.3.3.2 Determining the detection efficiency mathematically using a pre-calibration of the detector

As a general rule, pre-calibration means the efficiency of a detector as determined by the manufacturer. Pre-calibration is carried out with traceable activity standards in a sufficient spatial region around the detector. For this purpose, a sufficient number of representative calibration points must be available. These site-dependent detection efficiencies are made available in the form of a file.

Based on this file, the user calculates the detection efficiencies of his/her own measurement geometries by means of the software program provided by the manufacturer. To describe the geometry of the counting source, a number of standard geometries such as boxes and cylinders are available to the user (see Figure 11). In addition, very complex (mostly rotationally symmetrical) geometries may also be defined.

To describe the counting source exhaustively, also includes its type and composition as well as its density. Possible absorbers between the counting source and the detector, such as source holders, may also be defined. With the aid of these indications, it is possible to calculate the detection efficiency as a function of the gamma-ray energy for any desired energy in the range from 10 keV to 7000 keV.

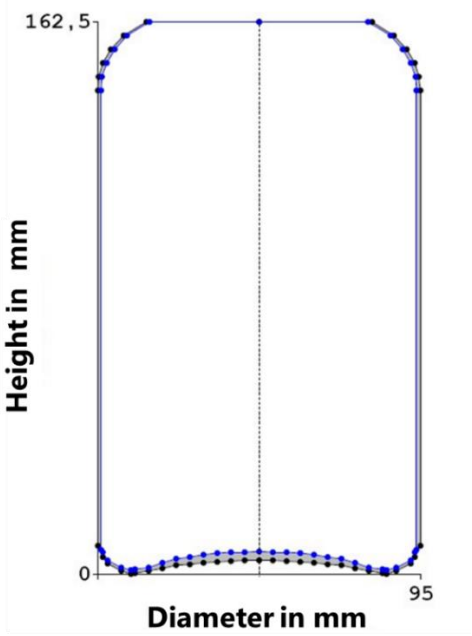

Fig. 10: Model of a 1 litre wide-mouth plastic bottle; inner outline (blue) and outer outline (black).

The typical standard uncertainties after pre-calibration listed in Table 1 were obtained from comparisons between measured and mathematically estimated detection efficiencies for different energy regions [9, 10].

Tab. 1: Typical standard uncertainties of the detection efficiencies according to the pre-calibration according to [9, 10]

Energy of the gamma-rays E_γ in keV	$E_\gamma \leq 150$	$150 < E_\gamma \leq 400$	$400 < E_\gamma \leq 1000$	$E_\gamma > 1000$
Recommended standard uncertainty in %	10	8	6	4

In addition to the mentioned standard uncertainties of the detection efficiencies from the pre-calibration, further uncertainty contributions from the exhaustive description of the counting source must be taken into account.

Moreover, in particular cases (e. g. in the case of particularly small sources located close to the detector such as press cakes placed directly on the detector end cap), an uncertainty contribution from 5 % to 10 % must be taken into account. The combined standard uncertainty may also be considerably higher than the values from Table 1 for sources with a very strong self-absorption.

6.3.3.3 Determining the detection efficiency mathematically according to the "detection efficiency transfer" principle

The detection efficiency transfer principle is based on the following: detection efficiencies $\varepsilon_{\mathrm{P}}(E)$ of a measurement geometry that have not be calibrated are estimated from experimentally determined, energy-dependent detection efficiencies $\varepsilon_{\mathrm{Ref}}(E)$ of a reference geometry without further measurements. Hereby, both the calibration sources and the counting sources can be described among their shape (e. g. diameter or height and/or density) also regarding chemical composition.

Software packages are available for the required calculations. These packages provide the average effective solid angles $\bar{\Omega}_{\mathrm{Ref}}(E)$ and $\bar{\Omega}_{\mathrm{P}}(E)$ for both measurement geometries by means of MC simulations (see Section 6.3.3.1). The required detection efficiency of the non-calibrated measurement geometry is calculated according to Equation (33):

$$\varepsilon_{\mathrm{P}}(E) = \varepsilon_{\mathrm{Ref}}(E) \cdot \frac{\bar{\Omega}_{\mathrm{P}}(E)}{\bar{\Omega}_{\mathrm{Ref}}(E)} \tag{33}$$

Since both geometries are based on identical detector properties, their uncertainty contributions to the uncertainties of the average effective solid angle largely cancel each other out. The standard uncertainty of the detection efficiency of the measurement geometry $\varepsilon_{\mathrm{P}}(E)$ is thus mainly determined by the experimentally determined standard uncertainty of the detection efficiency of the reference geometry $\varepsilon_{\mathrm{Ref}}(E)$ [11].

Compared to the procedure described in Section 6.3.3.2, this procedure yields smaller uncertainties for the detection efficiency of the non-calibrated measurement geometry [12, 13].

7 Correction of coincidence summations

7.1 Fundamentals

When radionuclides decay, in many cases, the nucleus of the progeny emits more than one gamma photon. These photons can be emitted so fast one after another that the gamma spectrometric measurement system only registers them as being simultaneous emitted, i. e. as coincident. The decay scheme of Y-88 shown in Figure 12 explains this effect in more detail.

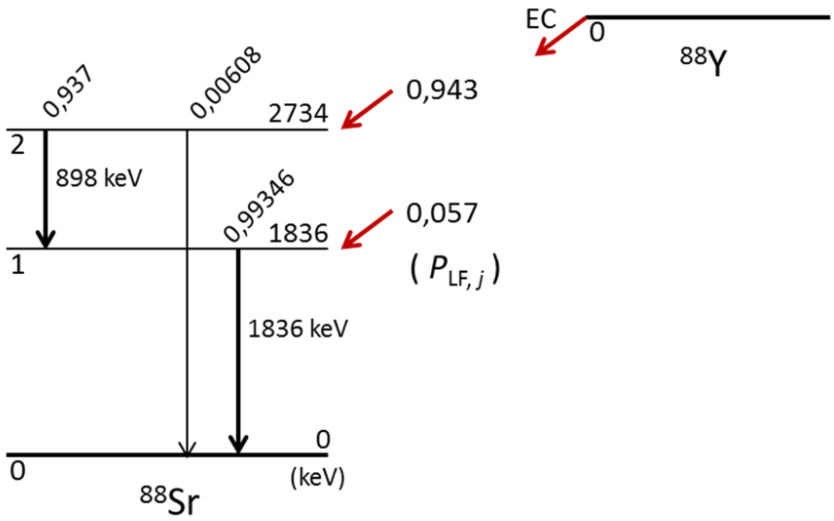

Fig. 11: Decay scheme of Y-88 after electron capture (EC).
The tilted figures represent the values of the gamma emission intensities of the level transitions 1 and 2, respectively, to the ground level 0.

If the photons with the energies E_1 = 898 keV and E_2 = 1836 keV reach the detector at the same time and there undergo interactions with the detector, the electronic unit may no longer be able to resolve them temporally. The closer the source is placed to the detector, the higher the probability of detecting several photons simultaneously. These signals are therefore not registered at the expected energy peaks E_1 and E_2, so that a loss in count rate occurs at both gamma peaks, which is also called "summing out". This summing out must be corrected if the detector has not been calibrated for specific nuclides.

Besides summing out, an increase of the pulse rate, or "summing in", may occur in another gamma peak of the radionuclide considered. A typical example is that of the radionuclide Ba-133 in the case of the three gamma peaks at the energies E_1 = 81,0 keV, E_2 = 302,9 keV, and E_3 = 383,9 keV. By summation of the photons with the energies E_1 and E_2, further counts are assigned to the gamma peak of Ba-133 at the energy E_3.

In addition, summation effects may cause gamma peaks that do not correspond to any transition in the decay scheme of the radionuclide considered to occur in the pulse height spectrum (see also Section 5.2). This is the case, for example, with the radionuclide Cs-134 with which, due to summation of the photons with the energy E_1 = 604,7 keV and E_2 = 795,9 keV, a summation peak with the energy at 1400,6 keV occurs in the pulse height spectrum.

Annex D provides a more detailed consideration of the mathematical fundamentals; additional information about summation and escape peaks can also be found in the General Chapter γ-SPEKT/SUMESC of this Procedures Manual.

7.2 Correction factors for coincidence summations $f_{1,j}$

The prerequisite for the correction of losses due to summing out is to know the total detection efficiency as a function of the energy $\varepsilon_t(E)$, which is determined ideally by means of radionuclides that only emit mono-energetic gamma-rays. These measurements take the total number of all the counts registered in the pulse height spectrum into account [14, 15]. Figure 13 shows an example of total detection efficiency.

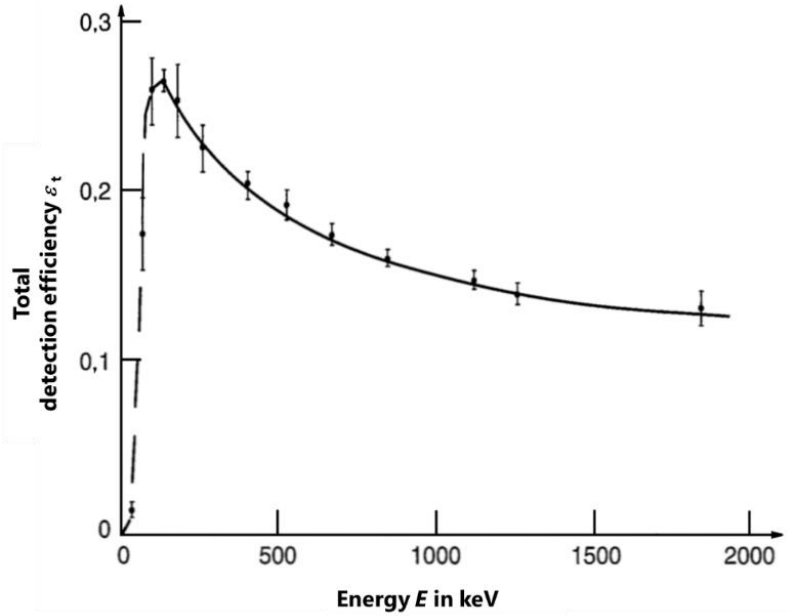

Fig. 12: Total detection efficiency ε_t as a function of the energy E for a p-type Ge detector (relative responsivity: 12 %) with a point-like source positioned very close to the detector end cap, according to [2].

As an alternative, it is also possible to express the total detection efficiency as the energy-dependent ratio of the full energy peak efficiency to the peak-to-total ratio (P/T). Hereby, the P/T ratio is the ratio of the number of counts in the gamma peak considered to the total number of counts registered in the pulse height spectrum up to the energy of the gamma peak considered [2, 3].

The total detection efficiency as a function of the gamma energy and the P/T ratio can also be determined by means of the mathematical procedure described in Section 6.3.3 if the required input quantities for the measurement geometry at hand are known.

For the simplest case, the correction factor $f_{1,j}$ for a coincidence summation in the gamma peak j considered may be calculated according to Equation (34) (see Annex D)

$$f_{1,j} = \frac{1}{1 - z \cdot \varepsilon_t} \tag{34}$$

where the factor z depends on the decay scheme of the radionuclide.

Note:
Equation (34) only applies to point-like sources. Volume sources require an additional averaging of the correction factors considering the volume of the counting source (see Equation (D17) in Annex D1).

When determining the correction factors experimentally, activity standards of radionuclides in accordance with Section 6.3.2.2 are normally used. The peak detection efficiencies obtained, as shown in Figure 14, are represented as double logarithmic plot. This allows the full energy peak detection efficiencies of single-line radionuclides with energies of more than 500 keV to be described in good approximation by fitted empirical functions. Due to summation effects, the full energy peak detection efficiencies of multi-line radionuclides deviate from the regression curve.

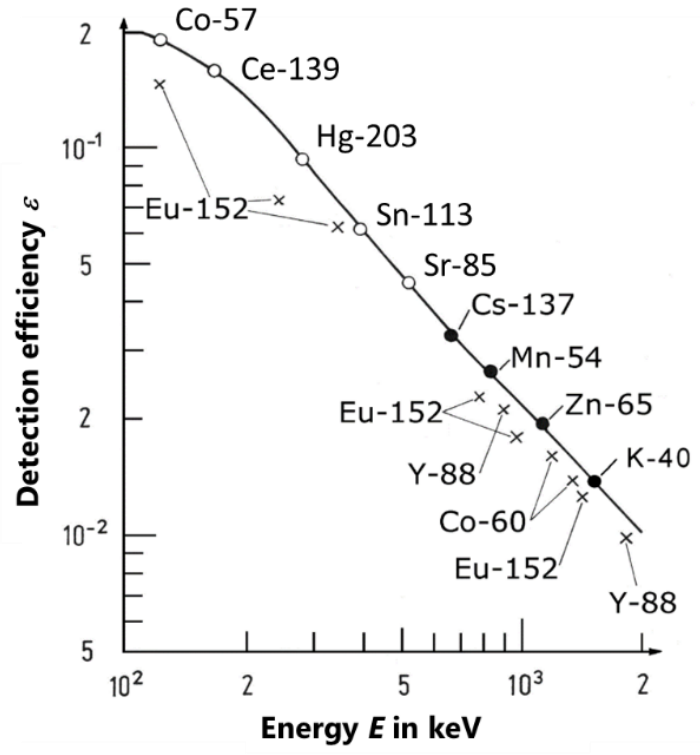

Fig. 13: Full energy peak detection efficiencies without taking summation corrections into account; according to [2]:
○ Single-line radionuclides with energies of less than 500 keV;
● Single-line radionuclides with energies of more than 500 keV;
× Multi-line radionuclides.

The correction factor for a gamma energy E can be determined from the values of the full energy peak detection efficiency according to Equation (35):

$$f_{1,E} = \frac{\varepsilon_{\mathrm{a}}}{\varepsilon_{\mathrm{exp}}} \tag{35}$$

where

ε_{a} full energy peak detection efficiency at the energy E, determined from the best-fit line;

$\varepsilon_{\mathrm{exp}}$ full energy peak detection efficiency of the multi-line radionuclide r at the energy E.

Note:
The correction factor determined according to Equation (35) applies to volume sources.

In case of radionuclides such as Ba-133, which emit both, gamma-ray photons and X-ray photons, coincidences also occur between the two different types of photons. These coincidences must also be corrected if the measurements are carried out with detector systems that are very sensitive in the low-energy region.

Commercially available software solutions are available for radionuclides with a complex decay scheme and for large-volume sources.

Typical approach to the software-aided determination of correction factors:

— The interesting radionuclides and the associated emission peaks are selected for which the summation corrections are to be calculated.

— Based on the radionuclide database included in the software, all possible combinations (cascades) of the gamma peaks considered are determined with other gamma peaks and X-ray peaks of the same radionuclide that may contribute to summing out or summing in. Hereby, two-, three- and manifold coincidences are taken into account. The software computes the probability of occurrence of each combination and archives the data in a file [15].

— Then, the MC simulation starts to compute the detection efficiency taking the summation effects into account and without taking them into account. The quotient of the two detection efficiencies thus calculated is the required summation correction.

In bottle and Marinelli beaker geometries, the corrections are between 5 % and 10 % when measuring radionuclides such as Co-60, Y-88, Cs-134 and Eu-152. In contrast, with point-like and surface sources lying directly on the detector, the corrections are in the order of 20 % to 50 %, which can be reduced by increasing the distance between the counting source and the detector. In the case of borehole detectors, the summation corrections may reach 500 % due to their high total detection efficiency.

Table 2 lists examples of correction factors $f_{1,j}$ for a number of radionuclides with diverse measurement geometries and types of detectors; for further examples it is referred to the literature [6]. A selection of frequently occurring summation peaks can also be found in the General Chapter γ-SPEKT/SUMESC of this Procedures Manual.

Tab. 2: Examples of the order of magnitude of the correction factors $f_{1,j}$ according to [2, 16].

Measurement geometries:

1 point-like source at a distance of 16 cm from the detector;
2 point-like source on the detector end cap;
3 1 litre bottle (90 mm in diameter) on the detector end cap;
4 1 litre Marinelli beaker
(thickness of the ring layer: approx. 25 mm; inner diameter: 88 mm);
5 0,45 litre Marinelli beaker
(thickness of the ring layer. approx 15 mm; inner diameter: 80 mm);

Detector types:

A n-type Ge detector; relative responsivity: 12,5 %;
B n-type Ge detector; relative responsivity: 25 %.

Radionuclide	**Energy**	$f_{1,j}$						
	in keV	**A1**	**A2**	**A3**	**A4**	**A5**	**B1**	**B2**
Co-60	1173	1,003	1,163	1,033	1,039	1,053	1,003	1,169
	1332	1,003	1,171	1,034	1,041	1,054	1,004	1,175
Y-88	898	1,003	1,154	1,029	1,035	1,046	1,005	1,374
	1836	1,003	1,178	1,035	1,049	1,067	1,006	1,403
Ba-133	81	1,005	1,300	1,054	1,052	1,071	1,008	1,684
	276	1,003	1,274	1,028	1,038	1,052	1,09	2,297
	303	1,002	1,161	1,015	1,020	1,027	1,008	2,054
	356	1,001	1,128	1,012	1,017	1,023	1,006	1,693
	384	0,999	0,906	0,989	0,985	0,977	1,000	1,169
Cs-134	605	1,004	1,252	1,050	1,063	1,085	1,005	1,249
	796	1,005	1,265	1,049	1,055	1,075	1,005	1,258
	1365	0,997	0,839	0,980	0,975	0,962	0,994	0,761
Eu-152	122	1,004	1,262	1,053	1,058	1,077	1,008	1,648
	245	1,006	1,434	1,072	1,088	1,122	1,011	2,086
	344	1,003	1,146	1,031	1,037	1,050	1,003	1,145
	411	1,007	1,424	1,071	1,075	1,103	1,008	1,432
	444	1,008	1,378	1,063	1,077	1,106	1,013	2,373
	779	1,004	1,249	1,042	1,045	1,062	1,005	1,256
	964	1,003	1,249	1,034	1,045	1,064	1,006	1,438
	1085	0,999	0,940	0,994	0,992	0,987	1,001	1,177
	1112	1,002	1,182	1,025	1,035	1,050	1,006	1,709
	1408	1,003	1,208	1,027	1,038	1,054	1,007	1,740

8 Self-attenuation correction

A considerable problem when determining the activity in large-volume sources is that they often have a different chemical composition and, in particular, a different density than the calibration source. For this reason, the gamma-rays are attenuated differently in the calibration source and in the counting source, which requires corrections.

The linear attenuation coefficient μ_s or the mass attenuation coefficient $\mu_s \cdot \rho^{-1}$ are used to describe self-attenuation [2, 17]. The linear attenuation coefficient μ_s characterizes the probability with which a gamma photon interacts with the atoms of the absorber material per centimetre of absorber thickness; it is stated in the unit m^{-1} or cm^{-1}. Since the linear attenuation coefficient is proportional to the density of a material, the mass attenuation coefficient $\mu \cdot \rho^{-1}$, which refers to the density ρ of the material, is commonly used; it is usually stated in the unit $cm^2 \cdot g^{-1}$.

Equation (36) applies to the average linear self-attenuation coefficient of a given source to be measured that consists of mass fractions r_i of different substances/elements:

$$\mu_{\mathrm{att}} = \bar{\mu} = \frac{\sum r_i \cdot \mu_i}{\sum r_i} \tag{36}$$

If a calibration source consists of material A, but the counting source consists of material B, the correction factor f_2 taking the self-attenuation differences into account is calculated according to Equation (37) according to the detection efficiency transfer principle (Sections 4 and 6.3.3.3):

$$f_2 = \frac{f_{\mathrm{s}}(\mathrm{B})}{f_{\mathrm{s}}(\mathrm{A})} = \frac{\bar{\Omega}_{\mathrm{B}}}{\bar{\Omega}_{\mathrm{A}}} \tag{37}$$

Commercially available software computes the attenuation correction factors according to Equation (37) if the mass fractions of the main elements or, ideally, the chemical composition of the counting source are known [18, 19]. Attenuation coefficients from the literature [17, 20] are used as a basis.

At photon energies less than 100 keV, this effect is particularly pronounced. It is therefore absolutely indispensable to apply a correction when determining the activity of I-129, Pb-210 or Am-241 among others. Above 100 keV, the effect has less significance. In this context, please refer to the procedure G-γ-SPEKT-FISCH-01. The literature [21, 22] provides sets of tables compiling average elemental compositions of different matrices.

9 Activity determination

The activity of a radionuclide is determined differently for single-line and multi-line radionuclides. Section 9.1 and 9.2 describe in more detail how the activity of single-line radionuclides is calculated. Determining the activity of multi-line radionuclides is more complex (see Sections 9.8 and 9.9). When determining radioactive substances in the environment, it is mostly the related activity, e. g. volume-related or mass-related, resulting from the activity measured in the counting source. In addition, the measurement uncertainty must also be stated.

Depending on the application at hand, diverse corrections (such as the pile-up, dead-time and decay corrections as well as the background contributions, interferences or the summation and escape peaks) must be taken into account when determining the activity. These topics will be described in more detail in the following sections.

9.1 Activity determination after nuclide-specific calibration

The activity A of a radionuclide is calculated according to Equation (38) after nuclide-specific calibration (see Section 6.3.1):

$$A = \frac{N_\mathrm{n} \cdot f_2}{\varepsilon_\mathrm{r} \cdot t_\mathrm{m}} \tag{38}$$

where

N_n net count number in the peak of the pulse height spectrum considered;

f_2 correction factor for self-attenuation differences (see Section 8);

ε_r detection efficiency for radiation of the energy considered in the full energy peak, in $\mathrm{Bq^{-1} \cdot s^{-1}}$;

t_m duration of measurement, in s.

The so-called live time must be used as the duration of measurement.

9.2 Activity determination after energy-specific calibration

The activity A of a radionuclide is calculated according to Equation (38) after nuclide-specific calibration (see Section 6.3.1):

$$A = \frac{N_\mathrm{n} \cdot f_1 \cdot f_2}{\varepsilon_\mathrm{r} \cdot p_\gamma \cdot t_\mathrm{m}} \tag{39}$$

where

p_γ emission intensity for the gamma-rays considered;

f_1 correction factor for summation effects (see Section 7).

9.3 Pile-up and dead-time correction

The electronic unit requires a minimal duration to process the signal of a voltage pulse (see Section 2.3). If another voltage pulse occurs during this time duration, this causes an increase in the voltage pulse still being processed, a so-called piling-up. This means that the two pulses registered at the same time are then missing in the gamma peaks of their photon energies in the pulse height spectrum: this is designated as pile-up losses. Instead, the summing pulse of a higher photon energy is assigned to these two pulses [1, 3]. Modern electronic units reject pile-up effects up to a certain extent (see Note in Section 9.4.1).

The total signal processing duration during a measurement is called dead time. As a rule, it increases with increasing count rate. This dead time must therefore be taken into account by subtracting it from the real time (dead-time correction). The duration of measurement t_m thus obtained is called live time; it is used for the evaluation.

With older spectrometric measurement systems that may not apply dead-time corrections automatically, these losses can be determined by means of a pulse generator running in parallel during the measurement [2, 23].

9.4 Decay corrections

9.4.1 Correction for the radioactive decay during the measurement

When measuring short-lived radionuclides with half-lives t_r that are comparable to or smaller than the duration of measurement, t_m, the decay of the radionuclide to be determined must be taken into account during the measurement. For this purpose, the right sides of Equations (38) and (39) must be multiplied by the decay correction factor to be calculated according to Equation (40):

$$f_3 = \frac{\frac{\ln 2}{t_\mathrm{r}} \cdot t_\mathrm{m}}{1 - \mathrm{e}^{\left(-\ln 2 \cdot \frac{t_\mathrm{m}}{t_\mathrm{r}}\right)}} = \frac{\lambda_\mathrm{r} \cdot t_\mathrm{m}}{1 - \mathrm{e}^{(-\lambda_\mathrm{r} \cdot t_\mathrm{m})}} \tag{40}$$

The result obtained is the activity of the radionuclide at the beginning of the measurement. With λ_r being the decay constant of the radionuclide r

Note:
If higher activities prevail that lead to a significant increase of the dead time, considerable counting losses are to expect which can no longer be sufficiently corrected by the automatic dead time correction. At dead times of approx. 30 % onwards, the counting losses are so high that one can no longer expect quantitatively correct results. In such cases, the measurement must, for example, be carried out with smaller amounts of the sample or the distance between the sample and the detector must be increased.

9.4.2 Correction for the radioactive decay related to a reference time

During a time period t_A which is defined as a time period between a reference time, e. g. the moment of sampling, and the beginning of the measurement, the activity of the radionuclide r in the sample decays. The necessary decay correction is taken into account by an additional correction factor according to Equation (41) which is applied to the right sides of Equations (38) and (39):

$$f_4 = e^{\frac{\ln 2}{t_r} \cdot t_A} = e^{\lambda_r \cdot t_A} \quad (41)$$

9.4.3 Notes concerning decay corrections in parent-progeny relations

If the half-life of the progeny nuclide is considerably shorter than that of the parent nuclide and the reference time of the activities in an environmental sample far before the beginning of the measurement, the half-life of the parent nuclide must be used for the decay correction (see Section 5.2 and Annex E). Otherwise, the activity of the short-lived progeny nuclide would be significantly overestimated.

Parent-progeny examples that are relevant to the monitoring of radioactive substances in the environment, are:

— Te-132 (t_r = 3,2 d) / I-132 (t_r = 2,3 h), and

— U-238 (t_r = 4,47 · 10^9 a) / Th-234 (t_r = 24,1 d),

— Ra-228 (t_r = 5,75 a) / Ac-228 (t_r = 6,15 h), as well as

— further pairs from the natural decay chains.

9.5 Background subtraction

Background spectra must be regularly recorded to take background contributions from the environment and contaminations of the gamma spectrometric measurement system by natural or artificial radionuclides into account. The interval between background measurements depends on the type of the respective measurement task and on the measuring routine of the laboratory. The background count rate R_0 must be taken into account when evaluating the pulse height spectrum according to Section 5.

The duration of the background measurement should correspond at least to the duration of the measurement expected for the counting source. In addition, background measurements should be carried out with samples that have a similar composition and whose own activity is negligible, for example, with distilled water for aqueous samples.

For more details on the peaks occurring in the background pulse height spectrum and on the dependence of the background spectra on the type of detector or spectrometer are described in the General Chapter γ-SPEKT/NULLEF of this Procedures Manual.

9.6 Interferences

The gamma peaks of radionuclides with identical or very similar gamma-ray energies may interfere in pulse height spectra. This effect is called interference.

In principle, interfering gamma peaks can originate either from the radionuclide to be determined itself or from other radionuclides also contained in the counting source. The better the energy resolution of the Ge detector, the less interferences are likely to occur.

When gamma peaks of different radionuclides overlap which have further peaks in the pulse height spectrum, then undisturbed peaks should be used to calculate the activity of the radionuclide. The count rate fraction of the interesting radionuclide in the multiplet can be calculated and subtracted based on the activity determined from the undisturbed peaks and the known emission intensity.

Various types of disturbances are presented in the General Chapter γ-SPEKT/INTERF of this Procedures Manual.

9.7 Summation peaks and escape peaks

Besides the corrections for coincidence summations discussed in Section 7, further peaks may occur in a pulse height spectrum due to the pair production effect – so-called single escape peaks (SE) and double escape peaks (DE).

Pair production means the generation of an electron/positron pair which occurs due to the interaction between electromagnetic radiation whose energy E_γ is greater than 1022 keV and matter such as the detector material. At energies of more than 4000 keV, the pair production effect is the prevailing interaction process between gamma-rays and matter.

Positrons formed in the detector crystal recombine with an electron thereby emitting two gamma quanta diametrically, each with an energy of 511 keV. These gamma quanta may then either leave the detector or remain in the detector and become involved in further interactions. These interactions either lead to partial or to complete absorption of one or both of the gamma quanta:

If one of the two photons is not absorbed in the detector, another peak becomes visible at an energy which is obtained by subtracting the energy of 511 keV from the actual energy of this gamma peak ($E_{\mathrm{SE}} = E_\gamma - 511\ \mathrm{keV}$). This peak is called a single escape peak.

If none of the two photons is absorbed in the detector, another peak becomes visible at an energy which is obtained by subtracting twice 511 keV from the actual energy of this gamma peak ($E_{\mathrm{DE}} = E_\gamma - 1022\ \mathrm{keV}$). This peak is called a double escape peak.

Further interactions of gamma quanta with the detector material lead to the formation of X-rays that may appear as X-ray escape peaks in the pulse height spectrum ($E_{\mathrm{XE}} = E_{\gamma} - E_{\mathrm{X-Ray}}$).

Detailed explanations can be found in the literature [1]; a selection of typical summation and escape peaks is provided in the General Chapter γ-SPEKT/SUMESC of this Procedures Manual.

9.8 Determining the activity of multi-line radionuclides

Several procedures are available to determine the activity of radionuclides with several gamma peaks from a complex pulse height spectrum; these procedures are used when a decrease in the standard uncertainty of the activity – and thus of the detection limit – is expected.

Two of these procedures are presented in the following. One of them is the simple procedure of the weighted mean, which is limited to the case of interference-free peaks of a single radionuclide. The other method is the universal procedure with a linear equation system which can be applied both to one or several radionuclides with several gamma peaks which may interfere with each other.

9.8.1 Weighted mean of the activity

The weighted mean A_{r} of the activity of a radionuclide is calculated from the activity values of m individual peaks, which were determined according to Sections 9.2 to 9.7, according to Equation (42); the standard uncertainty of the weighted mean is calculated according to (43):

$$A_{\mathrm{r}} = \frac{\sum_{J=1}^{m} A_j \cdot w_j}{\sum_{J=1}^{m} w_j} \tag{42}$$

$$u(A_{\mathrm{r}}) = \sqrt{\frac{1}{\sum_{J=1}^{m} w_j}} \tag{43}$$

Hereby, a weighting factor w_j is assigned to each activity value A_j. The weighting factor is usually based on the standard uncertainty of the activity calculated from the individual peak and is calculated according to Equation (44).

$$w_j = \frac{1}{u^2(A_j)} \tag{44}$$

In this way, peaks with a small standard uncertainty are assigned more weight compared to peaks with a greater standard uncertainty.

To calculate the weighted mean, individual peaks are selected whose activities' standard uncertainties are of roughly the same order of magnitude. In this context, the following conditions must be met:

— no overlapping with other peaks, including background peaks;

— as far as possible: undisturbed spectrum continuum below the individual peak;

— correction of summation and self-attenuation effects (see Sections 7 and 8)

The approach to determining the weighted mean is described in detail in Annex B.

9.8.2 Evaluation with a linear equation system

In a spectrum with numerous radionuclides with each of them emitting several gamma photons, interferences (peak overlap) are bound to occur. In this case, the activities of radionuclides can only be calculated with more complex procedures such as that described below using matrix algebra.

In a pulse height spectrum with a total of n_{L} peaks, a number N of radionuclides are present with the sought activities A_r ($r = 1 \ldots N$; in the following, the list of the radionuclides considered in the pulse height spectrum will be called "nuclide list"). Suitable individual peaks belonging to this radionuclide r.

Note:
The criteria for selecting suitable individual peaks are an emission intensity of the gamma peak as high as possible as well as a contribution to interferences in the gamma peak considered as low as possible.

The net count rates of the gamma peaks $R_{\mathrm{n},k}$ ($k = 1 \ldots k_{\mathrm{L}}$; "List of peaks") are converted into pseudo-activities $\hat{A}_k$ according to Equation (45) by means of the detection probability ε_k and of the self-attenuation correction factor $f_{2,k}$:

$$\hat{A}_k = \frac{R_{\mathrm{n},k} \cdot f_{2,k}}{\varepsilon_k} \tag{45}$$

Several radionuclides may contribute to the pseudo-activity of the peak k, so that Equation (46) must be set up from the total number n_{L} of individual peaks for each peak k:

$$\hat{A}_k = \sum_{r=1}^{N} M_{k,r} \cdot A_r = M_{k,1} \cdot A_1 + M_{k,2} \cdot A_2 + \cdots + M_{k,N} \cdot A_N \tag{46}$$

The coefficients $M_{k,r}$ are the relation of the emission intensity $p_{\gamma,k,r}$ and the correction factor for summation effects $f_{1,k,r}$ of the individual peak k of the radionuclide r from the nuclide list; they are calculated according to Equation (47):

$$M_{k,r} = \frac{p_{\gamma,k,r}}{f_{1,k,r}} \tag{47}$$

The coefficients $M_{k,r}$ which do not contribute to the pseudo-activity of the peak k considered, are zeroed.

All equations determined according to Equation (46) yield a linear equation system which can be described as $\hat{\boldsymbol{A}} = \mathbf{M}\,\boldsymbol{A}$ in simplified matrix notation. The matrix **M** consists of n_{L} rows for the peaks k of the list of peaks and of N columns for the radionuclides of the list of nuclides.

The vector of the activities $\boldsymbol{A}$ and its covariance matrix $\mathbf{U_A}$ can be calculated from this equation system, using least-square procedures (as described in Annex C.5 of the literature [24]). From this, it is possible to read out the activities A_{r} and the assigned uncertainties $u(A_{\mathrm{r}})$. The standard uncertainties of the matrix elements $\mathrm{M}_{k,r}$ of the matrix **M** must be taken into account, depending on the application at hand.

This procedure is usually implemented in the gamma spectrometry software.

Note:

For a radionuclide r with a single gamma peak, which corresponds to the peak k in the spectrum and is available free of interferences, it is possible to separate Equation (46) from the linear equation system, which simplifies the matrix. In this way, the activity of the radionuclide r considered is yielded as:

$$A_{\mathrm{r}} = \frac{\hat{A}_r}{M_{k,r}} = \frac{R_{\mathrm{n},k} \cdot f_{1,k,r} \cdot f_{2,k}}{\varepsilon_k \cdot p_{\gamma,k,r}} \tag{48}$$

This equation corresponds to Equation (39) in Section 9.2.

9.9 Particularities when determining the activity of natural radionuclides

The General Chapter γ-SPEKT/NATRAD of this Procedures Manual provides details on the measurement of natural radionuclides. When determining the activity of natural radionuclides, their specific properties must always be taken into account. Moreover, disturbances of the radioactive equilibrium by physico-chemical processes of anthropogenic and geogenic origins must be identified and corrected correspondingly.

Three examples will be mentioned in the following:

— Example 1: *Volatility of radon*
  The volatility of radon is a metrological problem when measuring sources in which the radioactive equilibrium between a parent nuclide and progeny nuclides is a prerequisite. For progeny nuclides that originate in the decay of radon, realizing such a prerequisite is not always possible.

— Example 2: *Large number of gamma peaks, even at low photon energies*
  The numerous peaks generated by the radionuclides from the natural decay chains are sometimes also detected in the lower energy region of the pulse height spectrum. Here, it is essential to take coincidence summation corrections (see Section 7) and

self-attenuation corrections (see Section 8) into account in order to determine the activity correctly.

— Example 3: *Disturbances of the equilibrium relation between U-238 and Th-234*
This disturbance may occur in the context of water treatment. The deviation of the radioactive equilibrium of these two isotopes can be determined by means of time-delayed measurements – in the present case, after a period of 24 days (approx. one half-life of the short-lived daughter nuclide Th-234).

9.10 Related activity

The activity A_{r} of the radionuclide r measured in the counting source is then related to the sample characteristics. When referring to

— a volume, one speaks of the activity concentration c_{r},

— a mass, one speaks of specific activity a_{r},

— an area, one speaks of activity per area $a_{F,\mathrm{r}}$.

Besides the corrections already mentioned, further corrections that are independent of the measurement of the activity may have to be taken into account. Such corrections are known losses, e. g., when taking or preparing the sample. The equations to calculate the related activity of a radionuclide are given in the respective procedures provided in this Procedures Manual.

9.11 Measurement uncertainty

The activity or the related activity must be stated with an assigned uncertainty. Depending on the requirement, the uncertainty to be stated is the standard uncertainty or the expanded uncertainty. For the expanded uncertainty, the value of the standard uncertainty is multiplied by a factor k, usually k = 2 [25]. The main individual contributions entering the calculation of the standard uncertainty of the individual activity value are the following:

— the standard uncertainty of the net count rate, based on the standard uncertainties of the gross area or of the background area, or, in the case of a peak fit, the standard uncertainty of the fit, as well as contributions of the background subtraction;

— the standard uncertainties of the radionuclide data;

— the standard uncertainty of the detection efficiency ε taking all uncertainties of the input quantities used for calibration in accordance with Section 6.3 into account;

— the standard uncertainties of each of the correction factors f_1 to f_n;

— standard uncertainties related to the procedure used, such as the mass or the volume of the sample.

Commercially available spectrometry software provides the option of including these contributions to the calculation of the activity or the related.

10 Decision threshold and detection limit

The decision threshold and the detection limit are determined according to [24]. Fundamentals on this topic can also be found in the General Chapters ERK/NACHWEISGR-ISO-01 to ERK/NACHWEISGR-ISO-03 of this Procedures Manual.

For measurements of radioactive substances and the external dose within the scope of the Integrated Measurement and Information System (IMIS), the factors $k_{1-\alpha}$ = 3 and $k_{1-\beta}$ = 1,645 were defined for the quantiles of the standardized normal distribution for the error of the 1st type and for the error of the 2nd type.

Contrary to that, the German Nuclear Safety Standards Commission (in German: Kerntechnischer Ausschuss, KTA) stipulates the use of the factors $k_{1-\alpha} = k_{1-\beta}$ = 1,645.

When using commercially available spectrometry software, the default settings may have to be adjusted to these values.

Examples of determination of the decision threshold and detection limit are provided in Annex C.

Annex A
Determining the activity of a radionuclide by evaluating a single gamma peak

The fundamental principle to determine the activity of a radionuclide in fish ash by evaluating a single gamma peak will be described in the following. The corresponding worked example can be found in the procedure G-γ-SPEKT-FISCH-01.

If a gamma peak of the radionuclide r with the net count rate $R_{\mathrm{n,r}}$ has been detected, the specific activity a_{r} of the radionuclide r is calculated according to Equation (A1), in relation to the fresh mass (FM) of the fish sample and to the time of sampling:

$$a_{\mathrm{r}} = \varphi \cdot R_{\mathrm{n,r}} = \frac{f_1 \cdot f_3}{\varepsilon_{\mathrm{A}} \cdot p_{\gamma,\mathrm{r}} \cdot m_{\mathrm{A}} \cdot q_{\mathrm{F}}} \cdot \mathrm{e}^{\lambda_{\mathrm{r}} \cdot t_{\mathrm{A}}} \cdot R_{\mathrm{n,r}} \qquad \text{(A1)}$$

with

$$f_3 = \frac{\lambda_{\mathrm{r}} \cdot t_{\mathrm{m}}}{1 - \mathrm{e}^{-\lambda_{\mathrm{r}} \cdot t_{\mathrm{m}}}}$$

where

$R_{\mathrm{n,r}}$ net count rate of the peak of the radionuclide r, in s^{-1};
φ procedural calibration factor, in $Bq \cdot s \cdot kg^{-1}$;
f_1 correction factor for the coincidence summation;
f_3 correction factor for the decay of the radionuclide r during the measurement;
ε_{A} detection efficiency in ash, in $Bq^{-1} \cdot s^{-1}$;
$p_{\gamma,\mathrm{r}}$ emission intensity of the gamma peak of the radionuclide r;
m_{A} mass of the ash used for the measurement, in kg;
q_{F} ratio of the fresh mass to the ash mass;
t_{A} duration between the sampling and the beginning of the measurement, in s;
t_{m} duration of the measurement, in s;
λ_{r} decay constant of the radionuclide r, in s^{-1}.

The composition of the count rate for the peak of the radionuclide r is in accordance with Equation (A2):

$$R_{\mathrm{n,r}} = R_{\mathrm{g,r}} - R_{\mathrm{T,r}} - R_{0,\mathrm{r}} \qquad \text{(A2)}$$

where

$R_{\mathrm{g,r}}$ gross count rate of the peak of the radionuclide r, in s^{-1};

$R_{\mathrm{T,r}}$ peak spectrum continuum count rate on the gamma peak of the radionuclide r, e. g. as the trapeze spectrum continuum count rate, in s^{-1};

$R_{0,\mathrm{r}}$ net count rate of the peak of the radionuclide r from the background effect spectrum, in s^{-1};

The uncertainty of the net count rate $u(R_{\mathrm{n,r}})$ is determined according to Equation (A3), the associated coefficients μ_k according to Equation (A4):

$$u(R_{\mathrm{n,r}}) = \sqrt{\mu_0 \cdot R_{\mathrm{n,r}}^2 + \mu_1 \cdot R_{\mathrm{n,r}} + \mu_2} \tag{A3}$$

with the coefficients

$$\mu_0 = 0$$

$$\mu_1 = \frac{1}{t_{\mathrm{m}}} \tag{A4}$$

$$\mu_2 = \frac{R_{\mathrm{T,r}} + R_{0,\mathrm{r}}}{t_{\mathrm{m}}} + u^2(R_{\mathrm{T,r}}) + u^2(R_{0,\mathrm{r}})$$

When using a trapeze procedure (linear spectrum continuum), it is possible to represent the term for μ_2 according to Equation (A5):

$$\mu_2 = \frac{R_{\mathrm{T,r}}}{t_{\mathrm{m}}} \cdot \left(1 + \frac{b}{2 \cdot L}\right) + R_{0,\mathrm{r}} \cdot \left(\frac{1}{t_{\mathrm{m}}} + \frac{1}{t_0}\right) + \frac{R_{\mathrm{T},0,\mathrm{r}}}{t_0} \cdot \left(1 + \frac{b_0}{2 \cdot L_0}\right) \tag{A5}$$

where

t_0 duration of the measurement of the background effect spectrum, in s;

b, b_0 base width of the peaks of the sample spectrum and of the background spectrum, in channels;

L, L_0 number of channels by means of which the peak's spectrum continuum on either side of the peak is determined, for the sample spectrum and the background spectrum;

$R_{\mathrm{T},0,\mathrm{r}}$ background continuum count rate of the peak of the radionuclide r, e.g. as the trapeze spectrum continuum count rate, in s^{-1}.

Equation (A5) applies in very good approximation also to the empirically calculated spectrum continuum step function.

For the standard uncertainty of the net count rate $u(R_{\mathrm{n,r}})$, the following applies according to Equations (A3) to (A5):

$$u^2(R_{\mathrm{n,r}}) = \mu_1 \cdot R_{\mathrm{n,r}} + \mu_2 = \\ = \frac{R_{\mathrm{n,r}}}{t_{\mathrm{m}}} + \frac{R_{\mathrm{T,r}}}{t_{\mathrm{m}}} \cdot \left(1 + \frac{b}{2 \cdot L}\right) + R_{0,\mathrm{r}} \cdot \left(\frac{1}{t_{\mathrm{m}}} + \frac{1}{t_0}\right) + \frac{R_{\mathrm{T,0,r}}}{t_0} \cdot \left(1 + \frac{b_0}{2 \cdot L_0}\right) \tag{A6}$$

If no corresponding peak is available in the background spectrum, the last two terms of Equation (A6) are cancelled.

The relative standard uncertainty of the procedure-related calibration factor must be determined according to Equation (7); hereby, the uncertainties of the decay corrections are negligible:

$$u_{\mathrm{rel}}(\varphi) = \sqrt{u_{\mathrm{rel}}^2(f_1) + u_{\mathrm{rel}}^2(f_3) + u_{\mathrm{rel}}^2(\varepsilon_{\mathrm{A}}) + u_{\mathrm{rel}}^2(p_\gamma) + u_{\mathrm{rel}}^2(m_{\mathrm{A}}) + u_{\mathrm{rel}}^2(q_{\mathrm{F}})} \tag{A7}$$

The combined standard uncertainty of the specific activity $u(a_{\mathrm{r}})$ is calculated using Equation (A8):

$$u(a_{\mathrm{r}}) = \varphi \cdot R_{\mathrm{n,r}} \cdot \sqrt{u_{\mathrm{rel}}^2(\varphi) + u_{\mathrm{rel}}^2(R_{\mathrm{n,r}})} \tag{A8}$$

Annex B
Determining the activity of a radionuclide by evaluating several gamma peaks

The fundamental principle to determine the activity of a radionuclide in fish ash by evaluating several gamma peaks will be described in the following. It is based on calculating the weighted mean of the activity in accordance with Section 9.8.1. The corresponding worked example can be found in the procedure G-γ-SPEKT-FISCH-01.

If a number m of gamma peaks of the radionuclide r have been selected in accordance with the criteria stated in Section 9.8.1, the specific activity a_r of the radionuclide r is calculated according to Equation (B1), in relation to the fresh mass (FM) of the fish sample and to the time of sampling:

$$a_\mathrm{r} = \varphi_\mathrm{M} \cdot A_\mathrm{r} = \frac{\mathrm{e}^{\lambda_\mathrm{r} \cdot t_\mathrm{A}} \cdot f_3}{m_\mathrm{A} \cdot q_\mathrm{F}} \cdot A_\mathrm{r} \tag{B1}$$

where

$R_{\mathrm{n,r}}$ net count rate of the peak of the radionuclide r, in s^{-1};

φ_M procedural calibration factor, in kg^{-1};

f_3 correction factor for the decay of the radionuclide r during the measurement;

m_A mass of the ash used for the measurement, in kg;

q_F ratio of the fresh mass to the ash mass;

t_A duration between the sampling and the beginning of the measurement, in s;

λ_r decay constant of the radionuclide r, in s^{-1}.

Here, A_r is the activity at the time of the measurement calculated as the weighted mean from m gamma peaks,

$$A_\mathrm{r} = \frac{\sum_{J=1}^{m} A_j \cdot w_j}{\sum_{J=1}^{m} w_j} = u^2(A_\mathrm{r}) \cdot \sum_{j=1}^{m} \frac{A_j}{u^2(A_j)} \tag{B2}$$

where the standard uncertainty $u(A_\mathrm{r})$ is provided by Equation (B3):

$$u(A_\mathrm{r}) = \sqrt{\frac{1}{\sum_{J=1}^{m} w_j}} = \sqrt{\frac{1}{\sum_{J=1}^{m} \frac{1}{u^2(A_j)}}} \tag{B3}$$

Here, the index j counts the peaks. The activities A_j of the individual peaks are calculated analogically to Equation (A1):

$$A_j = \frac{R_{\mathrm{n},j} \cdot f_{1,j}}{\varepsilon_{\mathrm{A},j} \cdot p_{\gamma,j}} = R_{\mathrm{n},j} \cdot \varphi_j \tag{B4}$$

where

$R_{\mathrm{n},j}$ net count rate of the peak j, in s^{-1};

φ_j procedural calibration factor, in Bq·s;

$f_{1,j}$ correction factor for the coincidence summation of the peak j;

$\varepsilon_{\mathrm{A},j}$ detection efficiency of the peak j in ash in $Bq^{-1}{\cdot}s^{-1}$
(see procedure G-γ-SPEKT-FISCH-01, Section 4.2.3);

$p_{\gamma,j}$ emission intensity of the peak j.

The variances of A_j are calculated according to the following equation:

$$u^2(A_j) = u^2(R_{\mathrm{n},j}) \cdot \varphi_j^2 + R_{\mathrm{n},j}^2 \cdot u^2(\varphi_j) \tag{B5}$$

If the net count rates are determined according to the trapeze procedure, their standard uncertainties can be calculated according to Equation (A6). If, however, a peak fit was applied, the factor $(1 + b/2L)$, which characterizes the trapeze procedure in Equation (A6), changes into a factor f_{B}, which depends on the fitting procedure used, so the following applies:

$$u^2(R_{\mathrm{n},j}) = \frac{R_{\mathrm{n},j}}{t_{\mathrm{m}}} + \mu_{2,j} \tag{B6}$$

$$\mu_{2,j} = \frac{R_{\mathrm{T},j}}{t_{\mathrm{m}}} \cdot f_{\mathrm{B}} + R_{0,\mathrm{r}} \cdot \left(\frac{1}{t_{\mathrm{m}}} + \frac{1}{t_0}\right) + \frac{R_{\mathrm{T},0,\mathrm{r}}}{t_0} \cdot \left(1 + \frac{b_0}{2 \cdot L_0}\right) \tag{B7}$$

In principle, the factor f_{B} depends on the average height of the spectrum continuum for each channel below the peak and on the ratio

$$\frac{R_{\mathrm{n},j} \cdot t_{\mathrm{m}}}{\sqrt{R_{\mathrm{T},j} \cdot t_{\mathrm{m}}}}$$

If the net count rates are close to the detection limit or to the decision threshold, f_{B} can be approximated by a fixed value; in this context, see the worked example provided in procedure G-γ–SPEKT-FISCH-01, Section 5.2.2.

Finally, the standard uncertainty of the specific activity is calculated as follows:

$$u(a_{\mathrm{r}}) = \varphi_{\mathrm{M}} \cdot A_{\mathrm{r}} \cdot \sqrt{u_{\mathrm{rel}}^2(\varphi_{\mathrm{M}}) + u_{\mathrm{rel}}^2(A_{\mathrm{r}})} \tag{B8}$$

where

$$u_{\mathrm{rel}}(\varphi_{\mathrm{M}}) = \sqrt{u_{\mathrm{rel}}^2(m_{\mathrm{A}}) + u_{\mathrm{rel}}^2(q_{\mathrm{F}})} \tag{B9}$$

Note:
The calculations listed in this section are already too complex to be recalculated manually, so that the UncertRadio software is resorted to in the corresponding worked example (see procedure G-γ–SPEKT-FISCH-01, Section 5.2.2). This is necessary in particular because the case treated here already represents an application of the linear deconvolution, so that the decision threshold and the detection limit have to be determined iteratively.

Annex C
Calculating the decision threshold and detection limit using the example of determining the specific activities of Cs-134 and Cs-137 in fish

The decision threshold and the detection limit are calculated according to [24]. In the case of emitters with a single-line (see procedure G-γ-SPEKT-FISCH-01, Section 5.1.1), it is possible to explicitly state equations to calculate the decision threshold and the detection limit. For this purpose, an Excel file and a project file for the UncertRadio software (see procedure G-γ-SPEKT-FISCH-01, Sections 7.1 and 7.2) are available on the website of this Procedures Manual.

For emitters with several gamma peaks, these equations can now be solved with the aid of a computer (see procedure G-γ-SPEKT-FISCH-01, Section 5.1.2). For the calculation, a project file for the UncertRadio software is currently available on the website of this Procedures Manual (see procedure G-γ-SPEKT-FISCH-01, Section 7.2).

The worked examples on the equations described in the following can be found in the procedure G-γ-SPEKT-FISCH-01.

C.1 Calculating the decision threshold and detection limit for the specific activity of Cs-137

To calculate the detection limit $a_{\mathrm{r}}^{\#}$, the decision threshold of the specific activity of the radionuclide a_{r}^{*} is first determined according to Equation (C1):

$$a_{\mathrm{r}}^{*} = \varphi \cdot k_{1-\alpha} \cdot \sqrt{\mu_2} = \varphi \cdot k_{1-\alpha} \cdot \sqrt{\frac{1}{t_{\mathrm{m}}} \cdot \left(R_{\mathrm{T,r}} + R_{0,\mathrm{r}}\right) + u^2\left(R_{\mathrm{T,r}}\right) + u^2\left(R_{0,\mathrm{r}}\right)} \qquad \text{(C1)}$$

By means of this result, it is possible to calculate the detection limit $a_{\mathrm{r}}^{\#}$ according to Equation (C2):

$$a_{\mathrm{r}}^{\#} = \frac{a_{\mathrm{r}}^{*} \cdot \Psi}{\theta} \cdot \left[1 + \sqrt{1 - \frac{\theta}{\Psi^2} \cdot \left(1 - \frac{k_{1-\alpha}^2}{k_{1-\beta}^2}\right)}\right] \qquad \text{(C2)}$$

with the auxiliary quantities:

$$\theta = 1 - k_{1-\beta}^2 \cdot u_{\mathrm{rel}}^2(\varphi)$$

$$\Psi = 1 + \frac{k_{1-\beta}^2}{2 \cdot a_{\mathrm{r}}^*} \cdot \frac{\varphi}{t_{\mathrm{m}}}$$

where

$k_{1-\alpha}$ quantile of the standard normal distribution related to the error of the 1st type;

$k_{1-\beta}$ quantile of the standard normal distribution related to the error of the 2nd type.

C.2 Calculating the decision threshold and detection limit for the specific activity of Cs-134

The decision threshold for emitters with several peaks can also be calculated directly, whereas the subsequent calculation of the detection limit already requires iterations. For more details, please consult the General Chapter ERK/NACHWEISGR-ISO-01 of this Procedures Manual.

The decision threshold for the specific activity of Cs-134 is calculated according to Equation (C3):

$$a_{\mathrm{r}}^* = \varphi_{\mathrm{M}} \cdot k_{1-\alpha} \cdot u(A_{\mathrm{r}} = 0) = \varphi_{\mathrm{M}} \cdot k_{1-\alpha} \cdot \sqrt{\frac{1}{\sum_j \frac{1}{\varphi_j^2 \cdot \frac{R_{\mathrm{T},j}}{t_{\mathrm{m}}} \cdot f_{\mathrm{B}}}}} \tag{C3}$$

The detection limit for the specific activity of Cs-134 is estimated according to Equation (C4):

$$a_{\mathrm{r}}^{\#} \approx a_{\mathrm{r}}^* + k_{1-\beta} \cdot u\left(a_{\mathrm{r}}^{\#\prime}\right) \tag{C4}$$

with the iterated standard deviation $u\left(a_{\mathrm{r}}^{\#\prime}\right)$:

$$u\left(a_{\mathrm{r}}^{\#\prime}\right) = \sqrt{\left(\frac{a_{\mathrm{r}}^*}{k_{1-\alpha}}\right)^2 + \left[u^2(a_{\mathrm{r}}) - \left(\frac{a_{\mathrm{r}}^*}{k_{1-\alpha}}\right)^2\right] \cdot \frac{a_{\mathrm{r}}^{\#\prime}}{a_{\mathrm{r}}}} \tag{C5}$$

Annex D
Fundamentals of correction factors for coincidence summation

A general description of the coincidence summation corrections is given in Section 7. For the simplest case, the determination of a full energy peak efficiency as described in Section 6.3.3.1, a correction factor must be added to Equation (31). In this annex, the derivation of this correction factor is dealt with in detail via the example of a point-like source.

Note:
Information on the nucleus-specific data contained here are given in the General Chapter KERNDATEN of this Procedures Manual. For further explanations concerning the terms used in the following, please refer to the literature [27].

In this annex, the following nomenclature applies with regard to the indices used:

— The nuclear levels of the progeny – the radionuclide Sr-88 in Figure D1 – are designated with the letter j. The value $j = 0$ describes the ground state level. All other values of j refer to the excited levels.

— Transitions always connect two energy levels. Thus, the transition from the level $j = 2$ to the level $j = 1$, for example, is expressed by the index pair $(2 \rightarrow 1)$.

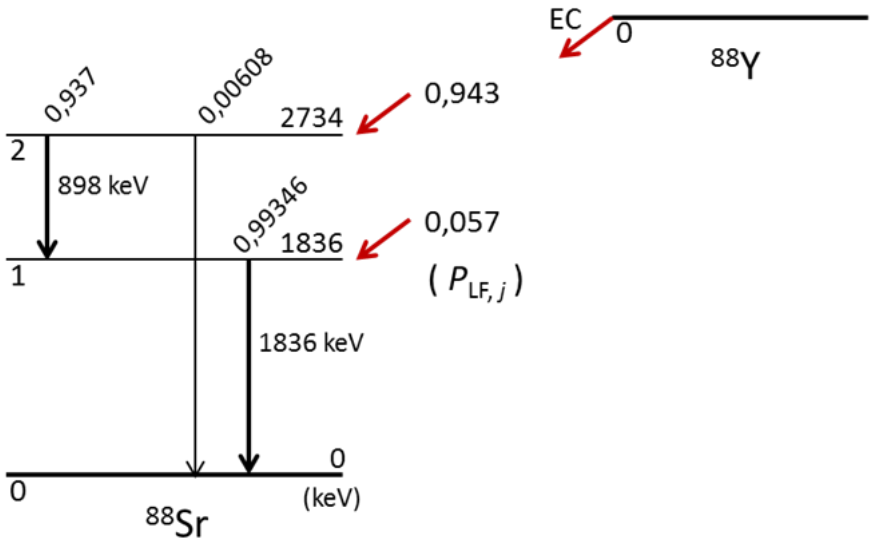

Fig. D1: Decay scheme of Y-88 after electron capture (EC).
The tilted numbers represent the values of the gamma emission intensities of the transitions 1 and 2, respectively, to the ground state level 0.
$P_{\mathrm{LF},j}$ is the probability for the nucleus level of the progeny to be populated after capturing electrons from the parent nuclide Y-88.

For a better understanding of the following sections, the most important symbols and their meaning are listed in Table D1.

Tab. D1: Symbols used in Annex D and their meaning

Symbol	Quantity	Symbol	Quantity according to [27]
$k \rightarrow l$	level transition from k to l		–
$p_{\gamma,k\rightarrow l}$	gamma emission intensity	I_{g}	gamma emission intensity
$p_{\mathrm{CE},k\rightarrow l}$	conversion electron emission intensity	I_{CE}	conversion electron emission intensity
$P_{\mathrm{g},k\rightarrow l}$	total transition probability for a gamma transition including conversion electrons	P_{g}	total transition probability for a gamma transition including conversion electrons
$\alpha_{\mathrm{t},k\rightarrow l}$	total internal conversion coefficient	α_{t}	total internal conversion coefficient
$x_{k\rightarrow l}$	branching ratio, defined by Equation (D4)		–
$x_{j,,,k}$	product of branching ratios of a transition sequence; defined by Equation (D6)		–
$P_{\mathrm{LF},j}$	level feeding probability for the level j due to nuclear transformation	$P_{\alpha}, P_{\beta}, P_{\gamma}$	transition probability for an alpha, beta or an electron capture transition feeding the level j
$P_{C,j}$	probability of a transition cascade; defined by Equations (D8) and (D9)		–
$P_{\mathrm{D,r}}(E)$	probability for detecting a count in the gamma peak at the energy E per decay of a radionuclide r		–
$\varepsilon_{\mathrm{p},k\rightarrow l}$	peak efficiency for a gamma photon		–
$\varepsilon_{\mathrm{t},m\rightarrow n}$	total efficiency for a gamma photon		–

D.1 Physical fundamentals

For a radionuclide with a complex decay scheme, the fundamentals of the effect of coincidence summation are explained for the simple case of a point-like source [26]. In the following, effects originating from X-rays will not be considered.

Following the nuclear transformation of the parent nuclide, the nuclear level j of the progeny nucleus is reached with a level feeding probability $P_{\mathrm{LF},j}$. Starting from this energy level, the atomic nucleus converts into the ground state level 0 in a cascade of extremely fast transitions. Various cascade paths through the level scheme are possible, since the transitions can, in principle, branch out from one level to the next lower one. The main difference between them is whether one or several gamma photons are emitted.

In the following, level transitions in which one gamma photon is emitted will be designated as $k \to l$ transition and such without photon emission will be designated as $m \to n$ transition. A gamma transition from a level j to a lower level i, with i being smaller than j, is characterized by emission of a gamma photon of the nucleus or of a conversion electron (CE) from the electron shell of the progeny. The sum of the two emission intensities is defined as the gamma transition probability $P_{\mathrm{g},k\to l}$ [27]:

$$P_{\mathrm{g},k\to l} = p_{\gamma,k\to l} + p_{\mathrm{CE},k\to l} \tag{D1}$$

where

$p_{\gamma,k\to l}$ emission intensity for gamma rays at the $k \to l$ transition;

$p_{\mathrm{CE},k\to l}$ emission intensity of the conversion electron at the $k \to l$ transition.

The total gamma conversion coefficient $\alpha_{\mathrm{t},k\to l}$ for the $k \to l$ transition is described in Equation (D2):

$$\alpha_{\mathrm{t},k\to l} = \frac{p_{\mathrm{CE},k\to l}}{p_{\gamma,k\to l}} \tag{D2}$$

The emission intensity for gamma-rays can thus be stated according to Equation (D3):

$$p_{\gamma,k\to l} = \frac{P_{\mathrm{g},k\to l}}{1+\alpha_{\mathrm{t},k\to l}} \tag{D3}$$

The factor $\left(1+\alpha_{\mathrm{t},k\to l}\right)^{-1}$ indicates the probability for a gamma photon to be emitted during a gamma transition.

If from a nuclear level k several transitions to different lower levels m (including l) take place, then the branching ratio $x_{k\to l}$ for the $k \to l$ transition is described by means of Equation (D4):

$$x_{k\to l} = \frac{P_{\mathrm{g},k\to l}}{\sum_m P_{\mathrm{g},k\to m}} \qquad \text{with} \qquad \sum_l x_{k\to l} = 1 \tag{D4}$$

The term stated in the denominator indicates the sum of the probabilities of all transitions originating from the level k. This sum is equated with the sum of the probabilities of those transitions with which the level k can be reached from levels $j \geq k$, i. e. after filling the levels $j \geq k$ by nuclear transitions and after subsequent transitions to the level k in the form of cascades. The equation reads:

$$\sum_m P_{\mathrm{g},k\to m} = \sum_{j\geq k} \left(P_{\mathrm{LF},j} \cdot x_{j,,,k}\right) \tag{D5}$$

Furthermore, Equation (D6) indicates – symbolically – the products of the branching probabilities, summed across a number of levels J_j of possible partial cascades leading from $j \geq k$ to k.

$$x_{j,,,k} = \sum_{J_j} x_{j,j-1} \cdot x_{j-1,j-2} \cdots x_{j-J_j,k} \tag{D6}$$

Hereby, $x_{j,,,0}$ = 1 applies to the ground state level k = 0 of the nucleus.

Apart from one exception, this means that starting from a level j, the ground state level is always reached via cascade transitions. This exception occurs when one of the levels within the cascade is metastable and the cascade is interrupted at this level.

From the Equations (D4) and (D5), the relation (D7) follows to calculate the gamma transition probability:

$$P_{\mathrm{g},k\to l} = x_{k\to l} \cdot \sum_{j\geq k} \left(P_{\mathrm{LF},j} \cdot x_{j,,,k}\right) \tag{D7}$$

Hereby, it becomes obvious that the $k \to l$ transition is contained in the total number of transitions $k \to m$.

If the level j is reached after a nuclear transformation, the probability of a cascade C running from this level to the ground state level 0 is designated as cascade probability $P_{C,j}$ whether gamma photons are emitted or not. This probability is calculated according to Equation (D8):

$$P_{C,j} = P_{\mathrm{LF},j} \cdot x_{j\to j-1} \cdot x_{j-1\to j-2} \cdots x_{1\to 0} \tag{D8}$$

If several partial cascades start from the same level j, i. e. if the cascade branches out, summation is carried out across these cascades, so that Equation (D9) applies

$$P_{C,j} = P_{\mathrm{LF},j} \cdot \sum_{\substack{m \\ (0<m<j)}} x_{j\to m} \cdot x_{m\to m-1} \cdot x_{m-1\to m-2} \cdots x_{1\to 0} = P_{\mathrm{LF},j} \cdot x_{j,,,k} = P_{\mathrm{LF},j} \qquad \text{(D9)}$$

Hereby, all branches, each of which may have originated from different levels, must be taken into account in Equation (D9).

In the following, the absolute probability $P_{\mathrm{D,r}}(E)$ that an event is registered in the gamma peak of the energy $E_{k\to l}$ in the pulse height spectrum per nuclear transformation of a radionuclide r, is derived explicitly. The product of $P_{\mathrm{D,r}}(E)$ by the activity A of the source yields the count rate to be expected in the gamma peak at the energy E.

Attention must be paid to the difference between this probability and the product $(\varepsilon_{\mathrm{p}} \cdot p_{\gamma})$ formed with the full energy peak efficiency. When defining the full energy peak detection efficiency ε_{p}, the only factor taken into account is whether a gamma photon from the nuclear transformation either reaches the detector and is detected there or not. In this context, the most important parameter is the geometry of the measuring arrangement. The probability $P_{\mathrm{D,r}}(E)$, however, additionally refers to the processes in the progeny nucleus following the nuclear transformation. A photon or several photons may be emitted in coincidence. The second case leads to modified count rates. The ratio $P_{\mathrm{D,r}}(E)$ to $p_{\gamma}(E)$ therefore represents an efficiency $\varepsilon(E)$. Its value deviates from $\varepsilon_{\mathrm{p}}(E)$ and is also called *apparent detection efficiency*.

$$\varepsilon_{\mathrm{p,app}}(E) = \frac{P_{\mathrm{D,r}}(E)}{p_{\gamma}(E)} \qquad \text{(D10)}$$

The starting point of the derivation of $P_{\mathrm{D,r}}(E)$ is Equation (D3). The emission intensity determined for gamma-rays $p_{\gamma,k\to l}$ according to Equation (D3) is now multiplied by detection efficiency $\varepsilon_{\mathrm{p},k\to l}$ of the gamma photon emitted at the $k \to l$ transition in the gamma peak at the energy $E_{k\to l}$. The product thus obtained is represented in Equation (D11):

$$p_{\gamma,k\to l} \cdot \varepsilon_{\mathrm{p},k\to l} = P_{\mathrm{g},k\to l} \cdot \frac{\varepsilon_{\mathrm{p},k\to l}}{1+\alpha_{\mathrm{t},k\to l}} = \frac{x_{k\to l}}{1+\alpha_{\mathrm{t},k\to l}} \cdot \varepsilon_{\mathrm{p},k\to l} \cdot \sum_{j\geq k} \left(P_{\mathrm{LF},j} \cdot x_{j,,,k}\right) \qquad \text{(D11)}$$

However, to detect this gamma photon in the gamma peak at the energy $E_{k\to l}$, the following condition must be met: no other gamma photons may be emitted from any other transitions from the same cascade. This means that the detection efficiency of the

gamma photon must be multiplied by the probabilities that no other gamma photon is emitted. This relation is described in Equation (D12):

$$P_{\mathrm{D,r}}(E) = \frac{x_{k\to l}}{1+\alpha_{\mathrm{t},k\to l}} \cdot \varepsilon_{\mathrm{p},k\to l} \cdot \sum_{j\geq k} \left(P_{\mathrm{LF},j} \cdot x_{j,,,k}\right) \cdot \prod_{\substack{m\to n \\ \neq k\to l}} \left[x_{m\to n} \cdot \left(1 - \frac{\varepsilon_{\mathrm{t},m\to n}}{1+\alpha_{\mathrm{t},m\to n}}\right)\right] \quad \text{(D12)}$$

where

$\varepsilon_{\mathrm{t},m\to n}$ total detection efficiency of a gamma photon at the $m \to n$ transition with the energy $E_{m\to n}$.

The index $m \to n \neq k \to l$ below the product symbol characterizes those cascade transitions in which no gamma photon is emitted.

The term $\varepsilon_{\mathrm{t},m\to n} \cdot \left(1+\alpha_{\mathrm{t},m\to n}\right)^{-1}$ is the probability for a gamma photon to be registered in the pulse height spectrum at the $m \to n$ transition at any point below the energy belonging to that transition. The probability that this photon is not registered corresponds to $1 - \varepsilon_{\mathrm{t},m\to n} \cdot \left(1+\alpha_{\mathrm{t},m\to n}\right)^{-1}$.

In Equation (D12), the factors $x_{j,,,k}$ and the product of factors $x_{m\to n}$, respectively, must be selected in a way that each transition occurs only once. Therefore, the products therein are replaced by single transition factors. This additional restriction of $j \geq k$ leads to equation (D13):

$$\begin{aligned} P_{\mathrm{D,r},C,j} &= P_{\mathrm{LF},j} \cdot x_{j\to j-1} \cdots x_{k\to l} \cdot x_{l\to l-1} \cdots x_{1\to 0} \cdot \frac{\varepsilon_{\mathrm{p},k\to l}}{1+\alpha_{\mathrm{t},k\to l}} \cdot \\ &\quad \cdot \prod_{\substack{m\to n \\ \neq k\to l}} \left[x_{m\to n} \cdot \left(1 - \frac{\varepsilon_{\mathrm{t},m\to n}}{1+\alpha_{\mathrm{t},m\to n}}\right)\right] = \\ &= P_{C,j} \cdot \frac{\varepsilon_{\mathrm{p},k\to l}}{1+\alpha_{\mathrm{t},k\to l}} \cdot \prod_{\substack{m\to n \\ \neq k\to l}} \left(1 - \frac{\varepsilon_{\mathrm{t},m\to n}}{1+a_{\mathrm{t},m\to n}}\right) \end{aligned} \quad \text{(D13)}$$

This equation must additionally be summed over the levels j and the possible paths C taken by the cascades from j via k and l to reach 0 in order to obtain Equation (D14) for calculating the desired probability $P_{\mathrm{D,r}}(E)$ (C depends on j)

$$P_{\mathrm{D,r}}(E) = \sum_j \sum_C \left[P_{C,j} \cdot \frac{\varepsilon_{\mathrm{p},k\to l}}{1+\alpha_{\mathrm{t},k\to l}} \cdot \prod_{\substack{m\to n \\ \neq k\to l}} \left(1 - \frac{\varepsilon_{\mathrm{t},m\to n}}{1+a_{\mathrm{t},m\to n}}\right)\right] \quad \text{(D14)}$$

If two or several photons are emitted at the same time within a cascade, the previous equation must be extended as follows:

$$P_{\mathrm{D,r}}(E) = \sum_{C,j} P_{C,j} \cdot \left[\prod_{k\to l}\left(\frac{\varepsilon_{\mathrm{p},k\to l}}{1+\alpha_{\mathrm{t},k\to l}}\right)\right] \cdot \left[\prod_{\substack{m\to n \\ \neq k\to l}}\left(1-\frac{\varepsilon_{\mathrm{t},m\to n}}{1+a_{\mathrm{t},m\to n}}\right)\right] \tag{D15}$$

In the pulse height spectrum, the product in the left square brackets represents the contribution of coincidentally emitted gamma photons to the gamma peak at the energy E; it is then interpreted as *summing in* if just the sum E corresponds to the energy of another transition. However, the probability for two gamma photons emitted at the same time to be detected by the detector is relatively small due to the multiplication of small full energy peak efficiencies.

$$E = \sum_{k\to l} E_{k\to l} \tag{D16}$$

The factors $\left[1-\varepsilon_{\mathrm{t},m\to n}\cdot\left(1+\alpha_{\mathrm{t},m\to n}\right)^{-1}\right]$ in Equation (D15) are smaller than 1. Their product thus reduces the probability of the photon to be detected, characterized by the product in the left square brackets. This effect is called *summing out*. As an illustration, one pretends a photon with the energy $E_{m\to n}$ were emitted at one of the $m\to n$ transitions. This would increase the pulse height of the photons of energy E assigned to the first factor by a fraction of the energy $E_{m\to n}$. This means that a count belonging to an increased pulse height would be registered above – and thus outside – the peak associated with E; therefore, it would be missing in the peak.

If a volume source rather than a point-like source is considered, then Equation (D15) must be averaged across the volume, resulting in Equation (D17):

$$P_{\mathrm{D,r}}(E) = \sum_{C,j}\left\{\frac{P_{C,j}}{V}\cdot\int_V\left[\prod_{k\to l}\left(\frac{\varepsilon_{\mathrm{p},k\to l}}{1+\alpha_{\mathrm{t},k\to l}}\right)\cdot\prod_{\substack{m\to n \\ \neq k\to l}}\left(1-\frac{\varepsilon_{\mathrm{t},m\to n}}{1+a_{\mathrm{t},m\to n}}\right)\right]\mathrm{d}V\right\} \tag{D17}$$

Calculating this equation requires advanced Monte Carlo procedures.

If the decay process also generates X-ray quanta, the structure of the relations explained here becomes considerably more complex.

D.2 Correction factors

In the case of a point-like source, the correction factor for coincidence summation for a considered gamma peak of the energy E is defined in Equation (D18):

$$f_E = \frac{\varepsilon_{\mathrm{p}}(E) \cdot p_{\gamma}(E)}{P_{\mathrm{D,r}}(E)} = \frac{\varepsilon_{\mathrm{p}}(E)}{\varepsilon_{\mathrm{p,app}}(E)} \tag{D18}$$

These equations will be used in the following to determine the correction factors for the radionuclides Co-60 and Y-88 whose progeny nuclei exhibit two nuclear levels above ground level in total.

In the case of Co-60, the decay nearly always leads to level 2, so that level 1 can only be reached from there. In this case, the correction factors are:

$$f_{E1} = f_{E,2\to1} = \frac{1}{1 - \frac{\varepsilon_{\mathrm{t},1\to0}}{1 + \alpha_{\mathrm{t},1\to0}}}$$
$$f_{E2} = f_{E,1\to0} = \frac{1}{1 - \frac{\varepsilon_{\mathrm{t},2\to1}}{1 + \alpha_{\mathrm{t},2\to1}}} \tag{D19}$$

In the case of Y-88, the decay leads with probabilities of 0,943 and 0,057 to level 2 and to level 1, respectively, which modifies the equation for f_{E2} (see Section 7.1 and the figure in Section D.3 on the next page):

$$f_{E1} = f_{E,2\to1} = \frac{1}{1 - \frac{\varepsilon_{\mathrm{t},1\to0}}{1 + \alpha_{\mathrm{t},1\to0}}}$$
$$f_{E2} = f_{E,1\to0} = \frac{1}{1 - \frac{P_{\mathrm{g},2\to1}}{P_{\mathrm{g},1\to0}} \cdot \varepsilon_{\mathrm{t},2\to1}} \tag{D20}$$

D.3 Worked example for Y-88

Taking the example of Y-88, determining the transition probabilities and the correction factors derived from them is shown by means of two occurring gamma peaks.

The nuclide-specific data available in the nuclide database for Y-88 are compiled Table D2, and the data derived from these are compiled in Table D3.

Tab. D2: Gamma data for Y-88 from the literature [27]

$k \rightarrow l$	P_{LF}	E in keV	P_q	$\alpha_{t,k\rightarrow l}$	$(1+\alpha_{t,k\rightarrow l})^{-1}$	p_γ
2 → 1	0,943	898,04	0,937	3,07E-04	0,99969	0,937
1 → 0	0,057	1836,07	0,9938	1,63E-04	0,99984	0,99346
2 → 0	0,943	2734,13	0,00608	1,24E-04	0,99988	0,00608

Tab. D3: Derived data for Y-88

$k \rightarrow l$	E in keV	$(1+\alpha_{t,k\rightarrow l})^{-1}$	$x_{k\rightarrow l}$	$\varepsilon_t(E)$
2 → 1	898,04	0,99969	0,937/(0,937+0,00608)=0,99355	0,094644
1 → 0	1836,07	0,99984	0,9938/0,9938=1,0	0,075176
2 → 0	2734,13	0,99988	0,00608/(0,937+0,00608)=0,0064470	

To better illustrate the worked example, the decay scheme of Y-88 from Figure D1 is shown again here:

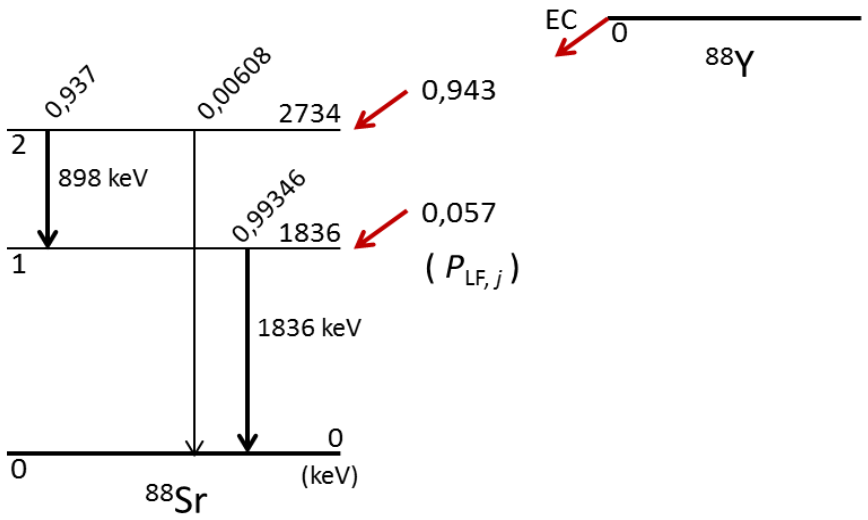

D.3.1 Correction factor for the 898 keV peak

In a pulse height spectrum, the photon from the 2 → 1 transition only shows up at the energy of 898 keV if the photon from the 1 → 0 transition has not been detected at the same time. The probabilities assigned to these two conditions are represented as a product in the following equation which is used to calculate the detection probability of the photon with the energy of 898 keV:

Level j = 2:

$$P_{\mathrm{D,Y-88}}(898) = \sum_{j=2}^{2}\left[P_{C,j}\cdot\prod_{k\to l=2\to 1}\left(\frac{\varepsilon_{\mathrm{p},k\to l}}{1+\alpha_{\mathrm{t},k\to l}}\right)\cdot\prod_{m\to n=1\to 0}\left(1-\frac{\varepsilon_{\mathrm{t},m\to n}}{1+a_{\mathrm{t},m\to n}}\right)\right] =$$

$$= P_{C,2}\cdot\frac{\varepsilon_{\mathrm{p},2\to 1}}{1+\alpha_{\mathrm{t},2\to 1}}\cdot\left(1-\frac{\varepsilon_{\mathrm{t},1\to 0}}{1+a_{\mathrm{t},1\to 0}}\right) = p_{\gamma,2\to 1}\cdot\varepsilon_{\mathrm{p},2\to 1}\cdot\left(1-\frac{\varepsilon_{\mathrm{t},1\to 0}}{1+a_{\mathrm{t},1\to 0}}\right)$$

In the present case, it is possible to describe the emission intensity of the gamma peak according to Equations (D3) and (D7) as follows:

$$p_{\gamma,2\to 1} = \frac{p_{\mathrm{g},2\to 1}}{1+\alpha_{\mathrm{t},2\to 1}} = \frac{x_{2\to 1}\cdot\sum_{j\geq k}\left(P_{\mathrm{LF},2}\cdot x_{2,,,1}\right)}{1+\alpha_{\mathrm{t},2\to 1}} = \frac{P_{\mathrm{LF},2}\cdot x_{2\to 1}\cdot x_{1\to 0}}{1+\alpha_{\mathrm{t},2\to 1}} = \frac{P_{C,2}}{1+\alpha_{\mathrm{t},2\to 1}}$$

The formula described in Equation (D20) for f_{E1} is obtained by inserting $P_{\mathrm{D,Y-88}}(898)$ into Equation (D18):

$$f_{898} = \frac{\varepsilon_{\mathrm{p}}(E)\cdot p_{\gamma}(E)}{P_{\mathrm{D,r}}(E)} = \frac{\varepsilon_{\mathrm{p}}(E)\cdot p_{\gamma}(E)}{p_{\gamma,2\to 1}\cdot\varepsilon_{\mathrm{p},2\to 1}\left(1-\frac{\varepsilon_{\mathrm{t},1\to 0}}{1+\alpha_{\mathrm{t},1\to 0}}\right)} =$$

$$= \frac{\varepsilon_{\mathrm{p}}(E)\cdot p_{\gamma}(E)}{p_{\gamma}(E)\cdot\varepsilon_{\mathrm{p}}(E)\left(1-\frac{\varepsilon_{\mathrm{t},1\to 0}}{1+\alpha_{\mathrm{t},1\to 0}}\right)} = \frac{1}{\left(1-\frac{\varepsilon_{\mathrm{t},1\to 0}}{1+\alpha_{\mathrm{t},1\to 0}}\right)}$$

With the values from the Tables D2 and D3, the value of the correction factor f_{898} amounts to:

$$f_{898} = \frac{1}{1-\frac{\varepsilon_{\mathrm{t}}(1836)}{1+\alpha_{\mathrm{t},1\to 0}}} = \frac{1}{1-\varepsilon_{\mathrm{t}}(1836)\cdot 0{,}99984} = \frac{1}{1-0{,}075176\cdot 0{,}99984}$$
$$= 1{,}0813$$

D.3.2 Correction factor for the 1836 keV peak

When calculating the correction factor for the 1836 keV peak, the detection probability of the photons with the energy of 1836 keV consists of two terms that represent the two cascades out of which the photons are emitted:

— Cascade 1 (term 1): The level j = 1 is populated directly when Y-88 decays. The transition thus takes place from 1 → 0.

— Cascade 2 (term 2): The level j = 2 is populated directly when Y-88 decays. The photon from the 1 → 0 transition at an energy of 1836 keV only shows up if the photon from the 2 → 1 transition has not been detected at the same time.

The following equation fully describes the detection probability $P_{\mathrm{D,Y-88}}(1836)$ as the sum of two terms:

$$P_{\mathrm{D,Y-88}}(1836) = \sum_{j=1}^{2}\left[P_{C,j}\cdot\prod_{k\to l=1\to 0}\left(\frac{\varepsilon_{\mathrm{p},k\to l}}{1+\alpha_{\mathrm{t},k\to l}}\right)\cdot\prod_{m\to n}\left(1-\frac{\varepsilon_{\mathrm{t},m\to n}}{1+a_{\mathrm{t},m\to n}}\right)\right]$$

The term for the level j = 1 is:

$$P_{\mathrm{D,Y-88}}(1836) = P_{C,1}\cdot\frac{\varepsilon_{\mathrm{p},1\to 0}}{1+a_{\mathrm{t},1\to 0}}$$

Note:
For j = 1, the factor in the second square brackets does not apply since level 2 is not involved in this case.

The term for the level j = 2 ($m \to n$ = 2 → 1) is:

$$P_{\mathrm{D,Y-88}}(1836) = P_{C,2}\cdot\frac{\varepsilon_{\mathrm{p},1\to 0}}{1+a_{\mathrm{t},1\to 0}}\cdot\left(1-\frac{\varepsilon_{\mathrm{t},2\to 1}}{1+a_{\mathrm{t},2\to 1}}\right)$$

The total detection probability $P_{\mathrm{D,Y-88}}(1836)$ is composed of

— the individual terms of the two energy levels,

— the relation $P_{C,j}$ and $P_{\mathrm{LF},j}$ according to Equation (D8),

— the relations $P_{\mathrm{g},j}$ and $P_{\mathrm{LF},j}$ according to Equation (D7).

$$P_{\mathrm{g},2\to 1} = P_{\mathrm{LF},2}\cdot x_{2\to 1}\cdot x_{1\to 0}$$

$$P_{\mathrm{g},1\to 0} = P_{\mathrm{LF},1}\cdot x_{1\to 0} + P_{\mathrm{LF},2}\cdot x_{2\to 1}\cdot x_{1\to 0}$$

$$P_{\mathrm{D,Y-88}}(1836) = P_{C,1}\cdot\frac{\varepsilon_{\mathrm{p},1\to 0}}{1+a_{\mathrm{t},1\to 0}} + P_{C,2}\cdot\frac{\varepsilon_{\mathrm{p},1\to 0}}{1+a_{\mathrm{t},1\to 0}}\cdot\left(1-\frac{\varepsilon_{\mathrm{t},2\to 1}}{1+a_{\mathrm{t},2\to 1}}\right) =$$

$$= \frac{\varepsilon_{\mathrm{p},1\to 0}}{1+a_{\mathrm{t},1\to 0}}\cdot\left[P_{C,1} + P_{C,2}\cdot\left(1-\frac{\varepsilon_{\mathrm{t},2\to 1}}{1+a_{\mathrm{t},2\to 1}}\right)\right] =$$

$$= \frac{\varepsilon_{\mathrm{p},1\to 0}}{1+a_{\mathrm{t},1\to 0}}\cdot\left[P_{\mathrm{LF},1}\cdot x_{1\to 0} + P_{\mathrm{LF},2}\cdot x_{2\to 1}\cdot x_{1\to 0}\cdot\left(1-\frac{\varepsilon_{\mathrm{t},2\to 1}}{1+a_{\mathrm{t},2\to 1}}\right)\right] =$$

$$= \frac{\varepsilon_{\mathrm{p},1\to 0}}{1+a_{\mathrm{t},1\to 0}}\cdot\left[P_{\mathrm{LF},1}\cdot x_{1\to 0} + P_{\mathrm{LF},2}\cdot x_{2\to 1}\cdot x_{1\to 0} - \frac{P_{\mathrm{LF},2}\cdot x_{2\to 1}\cdot x_{1\to 0}\cdot\varepsilon_{\mathrm{t},2\to 1}}{1+a_{\mathrm{t},2\to 1}}\right] =$$

$$= \frac{\varepsilon_{\mathrm{p},1\to 0}}{1+a_{\mathrm{t},1\to 0}}\cdot\left(P_{\mathrm{g},1\to 0} - P_{\mathrm{g},2\to 1}\cdot\frac{\varepsilon_{\mathrm{t},2\to 1}}{1+a_{\mathrm{t},2\to 1}}\right)$$

With $p_\gamma(E) = \frac{P_{g,1\to0}}{1+a_{t,1\to0}}$ and a number of transformations and replacements, the correction factor f_E from Equation (D18) becomes the correction factor in Equation (D20):

$$f_{1836} = \frac{\varepsilon_p(1836)\cdot p_\gamma(1836)}{P_{D,r}(1836)} = \frac{\varepsilon_p(1836)\cdot p_\gamma(1836)}{\frac{\varepsilon_{p,1\to0}}{1+a_{t,1\to0}}\cdot\left(P_{g,1\to0} - P_{g,2\to1}\cdot\frac{\varepsilon_{t,2\to1}}{1+a_{t,2\to1}}\right)} =$$

$$= \frac{\varepsilon_p(1836)\cdot\frac{P_{g,1\to0}}{1+a_{t,1\to0}}}{\frac{\varepsilon_p(1836)}{1+a_{t,1\to0}}\cdot\left(P_{g,1\to0} - P_{g,2\to1}\cdot\frac{\varepsilon_{t,2\to1}}{1+a_{t,2\to1}}\right)} = \frac{P_{g,1\to0}}{P_{g,1\to0} - P_{g,2\to1}\cdot\frac{\varepsilon_{t,2\to1}}{1+a_{t,2\to1}}} =$$

$$= \frac{P_{g,1\to0}}{P_{g,1\to0} - P_{\gamma,2\to1}\cdot\varepsilon_{t,2\to1}} = \frac{1}{1-\frac{P_{\gamma,2\to1}}{P_{g,1\to0}}\cdot\varepsilon_{t,2\to1}}$$

With the values from the Tables D2 and D3, the value of the correction factor f_{1836} amounts to:

$$f_{1836} = \frac{1}{1-\frac{0{,}937}{0{,}9938}\cdot 0{,}094644} = 1{,}098$$

Annex E
Utilization of special radionuclide libraries for natural radionuclides

When using gamma spectrometry, radionuclides of the natural decay chains that do not emit gamma-rays can, in certain cases, only be determined indirectly via their progeny products. In such measurements, the radioactive equilibrium between the parent nuclide and the progeny nuclides to be measured must be ensured.

In environmental samples, the radioactive equilibrium may be disturbed due to the different chemical and/or biochemical properties of the elements concerned. An example for this case is the different solubility of radium and thorium in water. In addition, the radioactive equilibrium may be disturbed – intentionally or inadvertently – during the sampling (e. g. by using filter materials) or due to radon escaping.

In the following, two examples will be used to explain why different half-lives are sometimes used for one and the same nuclide:

E.1 Considering the radionuclides Pb-214 and Bi-214

When using the radionuclides Pb-214 and Bi-214 to determine a parent nuclide, this needs to be based on different half-lives depending on the application (see Table E1). Therefore, it is necessary to generate a specific radionuclide library or each application:

— determining Ra-226;

— determining Rn-222 after separating it from Rn-222 and from its parent nuclide Ra-226;

— determining radon progenies in the absence of the parent nuclide Rn-222.

E.2 Considering the radionuclides Th-228 and Ra-224

Different activity concentrations of radium and thorium isotopes are encountered in aquatic systems. This is mainly due to their different chemical or biochemical properties, for example in deep water.

If the exact nuclide composition is to be determined in an aqueous solution at the time of sampling, the activity concentration must be determined in the sample soon after taking the sample since the radionuclide Ra-224 might otherwise decay due to its comparatively short half-life of 3,66 days. This radionuclide is preferably determined via its progeny nuclide Pb-212. In such a case, it would be advisable to generate a special

radionuclide library in which the half-life of Ra-224 amounting to 3,66 days is deposited for Pb-212. Since Th-228 may also be present in the aqueous solution, the same sample should be measured again after approx. 4 days and re-evaluated by means of the same radionuclide library. If, with reference to the sampling date, the same value is obtained within the limits of the measurement uncertainties, the radionuclide determined is Ra-224. In this case, the activity concentration of Th-228 lies below the decision threshold, which is usually the rule in deep water.

Tab. E1: The half-lives of Pb-214 and Bi-214 used for different applications in gamma spectrometry

Parent nuclide to be determined	via progeny nuclides	Half-life of the progeny nuclides from the radionuclide library	Time of measurement	Note	Typical counting source
Ra-226	Pb-214 Bi-214	1600 a	more than 20 days after filling the measurement container	test substance preferably in gas-tight measurement containers	environmental sample, direct; e. g. soil, sediments, construction material
Rn-222	Pb-214 Bi-214	3,8 d	no wait necessary prior to the measurement	reference indication: date and time of end of Rn-222 collection interruption-free Rn-222 collection, preferably for longer than 20 days under comparable conditions	activated carbon filter with sampled Rn-222
Pb-214 Bi-214	none	26,8 min 19,8 min	immediately after sampling	reference indication: date and time of end of the collection of radium progenies interruption-free collection, for at least 3 hours under comparable conditions	air filter with sampled radium progenies

Note:
If, against all expectations, a considerable increase (doubling of the value, for example) has been measured after four days, the value measured applies to the radionuclide Th-228 which, in turn, occurs in radioactive equilibrium with Ra-224. To determine Th-228 accurately, another radionuclide library must be used where the value for the half-life of Th-228 amounts to 1,91 years for the progeny nuclide Pb-212. The activity concentration determined applies both for Th-228 and for its progeny nuclide Ra-224.

After another 20 days, the radioactive equilibrium between the parent nuclide Th-228 and its progeny nuclide Ra-224 has been re-established, and the sample can be measured again if the activity concentration of Th-228 is a parameter of interest. When evaluating

the pulse height spectrum, the activity concentration of Th-228 is determined by means of the radionuclide Pb-212. In this case, the radionuclide library containing the half-life of Th-228 (1,91 years) must be used.

Note:

Besides the deviation of the radioactive equilibrium between Ra-224 and Th-228 discussed here, activity concentrations of Ra-228 to Th-228 deviating from the radioactive equilibrium are, as a rule, also encountered in aquatic systems.

In solid samples (soil, sediments, etc.), the radionuclides Th-228 and Ra-224 can be expected to occur in the radioactive equilibrium. Their activity concentrations are therefore determined by means of the radionuclide Pb-212, so that in this case, it is also necessary to use a radionuclide library listing the half-life of Th-228 as 1,91 years.

References

[1] Knoll, G. F.: *Radiation detection and measurement*. 4th Edition. New York: John Wiley & Sons Inc., 2010. ISBN 978-4-470-13148-0.

[2] Debertin, K., Helmer, R. G.: *Gamma- and X-Ray Spectrometry with Semiconductor Detectors*. Amsterdam: North Holland.1988. ISBN 978-0444871077.

[3] Gilmore, G.: *Practical Gamma-ray Spectrometry*. 2nd Edition. Chichester: John Wiley & Sons Ltd., 2008. ISBN 978-0-470-86196-7.

[4] IEC 60973:1989, *Test procedures for germanium gamma-ray detectors*.

[5] IEEE 325:1996, *Test procedures for germanium gamma-ray detectors*.

[6] Debertin, K., Schötzig, U.: *Bedeutung von Summationskorrektionen bei der Gamma-strahlen-Spektrometrie mit Germaniumdetektoren*. PTB-Ra-24, Braunschweig: PTB, May 1990.

[7] Helmer, R. G., Hardy, J. C., Iacob, V. E., Sanchez-Vega, M., Neilson, R. G., Nelson, J.: *The use of Monte Carlo calculations in the determination of a Ge detector efficiency curve*. Nucl. Instr. Meth. Phys. Res. A, 2003, Vol. 511, pp. 360 - 381.

[8] Venturini, L., Vanin, V.R.: *HPGe detector efficiency calibration for extended sources in the 50-1400 keV energy range*. Appl. Radiat. Isot., 1993, Vol. 44, Nr. 7, pp. 999 - 1002. ISSN 0969-8043.

[9] Venkataraman, R., Bronson, F., Atrashkevich, V., Young, B. M., Field, M.: *Validation of in-situ object counting system (ISOCS) mathematical efficiency calibration software*. Nucl. Instr. and Meth., 1999, A 422, p. 450.

[10] Bronson, F. L., Venkataraman, R,: *Validation of the Accuracy of the LABSOCS Mathematical Efficiency Calibration for Typical Laboratory Samples*. 46th Annual Conference on Bioassay, Analytical, and Environmental Radiochemistry, November 12 - 17, Seattle, 2000.

[11] Arnold, D., Sima, O.: *Transfer of the efficiency calibration of germanium gamma-ray detectors using the GESPECOR software*. Appl. Radiat. Isot., 2002 Vol. 56, Nr. 1 - 2, pp. 71 - 75. ISSN 0969-8043.

[12] Arnold, D., Sima, O.: *Extension of the efficiency calibration of germanium detectors using the GESPECOR software*. Appl. Radiat. Isot., 2004, Vol. 61, No. 2 - 3, pp. 117 - 121. ISSN 0969-8043.

[13] Sima, O., Arnold, D., Dovlete, C.: *GESPECOR: A versatile tool in gamma-ray spectrometry*. J. Radioanal. Nucl. Chem., 2001, Vol. 248, pp. 359-364. Available at: http://dx.doi.org/10.1023/A:1010619806898, [last accessed on 4 October 2017].

[14] Debertin, K., Schötzig, U.: *Coincidence Summing Corrections in Ge(Li)-Spectrometry at Low Source-to-Detector Distances*. Nucl. Instr. and Meth., 1979, Vol. 158, pp. 471 - 477.

[15] Arnold, D., Sima, O.: *Tool for processing decay data in view of coincidence summing calculations*. Appl. Radiat. Isot., 2008, Vol. 66, pp. 705 - 710. ISSN 0969-8043.

[16] Debertin, K.; Ren, J.: *Measurements of the Activity of Radioactive Samples in Marinelli Beakers*. Nucl. Instr. Meth. Phys. Res. A, 1989, Vol. 278, pp. 541 - 549.

[17] Hubbell, J. H.: *Photon Mass Attenuation and Energy-absorption Coefficient from 1 keV to 20 MeV*. Int. J. Appl. Radiat. Isot., 1982, Vol. 33, pp. 1269 - 1290.

[18] Arnold, D., Sima, O.: *Accurate computation of coincidence-summing corrections in low level gamma-ray spectrometry*. Appl. Radiat. Isot., 2000, Vol. 53. Nos. 1 - 2, pp 51 - 56. ISSN 0969-8043.

[19] Eckert & Ziegler Nuclitec GmbH, ed: *Calibration Standards and Instruments – Product Information*. 1st edition, 2009, p. 85. Available at: http://www.ezag.com.fileadmin/ezag/user-uploads/isotopes/pdf/Nuclitec_Isotrak_Catalog.pdf, [last accessed on 5 October 2017].

[20] Berger, M. J., Hubbell, J. H., Seltzer, S. M., Chang, J., Coursey, J. S., Sukumar, R., Zucker, D. S., Olsen, K.: *NIST Standard Reference Database 8 (XGAM)*. In: National Institute of Standards and Technology, ed.: XCOM: Photon Cross Sections Database [online]. Version: November 2010, available at: http://www.nist.gov/pml/data/xcom/index.cfm, [last accessed on 4 October 2017].

[21] Souci, S. W., Fachmann, W., Kraut, H.: *Lebensmitteltabelle für die Praxis*. *Der kleine Souci/Fachmann/Kraut.* 5th edition. Stuttgart: WVG, 2011. ISBN 978-3-8047-2679-6. Also available at: http://www.nutri-science.de/software/nutribase.php, [last accessed on 4 October 2017].

[22] Bosold, D., Pickhardt, R.: B1 – *Zemente und ihre Herstellung*. In: InformationsZentrum Beton GmbH, ed.: Zement-Merkblätter Betontechnik [online]. Version 9.2017, available at: https://www.beton.org/service/zement-merkblaetter/, [last accessed on 16 October 2017].

[23] Debertin, K.: *Messanleitung für die Bestimmung von Gammastrahlen-Emissionsraten mit Germaniumdetektoren*. PTB-Ra-12, Braunschweig: PTB September 1980.

[24] ISO 11929:2010, *Determination of the characteristic limits (decision threshold, detection limit and limits of the confidence interval) for measurements of ionizing radiation – Fundamentals and application.*

[25] JCGM-100:2008, *Evaluation of measurement data – Guide to the expression of uncertainty in measurement* (GUM). Available at:
http://www.bipm.org/en/publications/guides/gum.html,
[last accessed on 5 October 2017].

[26] Kanisch, G., Vidmar, T., Sima, O.: *Testing the equivalence of several algorithms for calculation of coincidence summing corrections*. Appl. Radiat. Isot., 2009, Vol. 67, No. 10, pp. 1952 - 1956. ISSN 0969-8043.

[27] Laboratoire National Henri Becquerel, ed: *Recommended Data* [online]. Version of 3 March 2017, available at: http://www.lnhb.fr/nuclear-data/nuclear-data-table/, [last accessed on 16 October 2017].